

WRDC-TR-90-3012



AD-A222 476

**Control of Orbiting Large
Space Structural Systems
with Discrete Time
Observational Data and
Random Measurement Noise**

**Dr. Peter M. Bainum
Prof. Xing Guangqian
Aprille J. Ericsson**

**Howard University
School of Engineering
Department of Mechanical Engineering
Washington, DC 20059**

March 1990

[Handwritten signature and date stamp]

Final Report for the Period July 1987 to February 1989

Approved for public release; distribution unlimited.

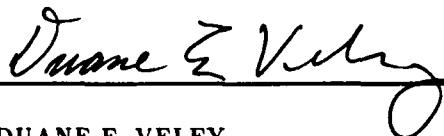
**FLIGHT DYNAMICS LABORATORY
WRIGHT RESEARCH AND DEVELOPMENT CENTER
AIR FORCE SYSTEMS COMMAND
WRIGHT-PATTERSON AIR FORCE BASE, OHIO 45433-6553**

NOTICE

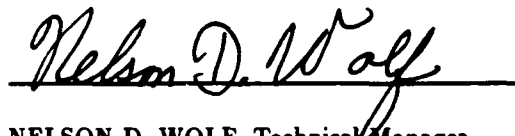
When Government drawings, specifications, or other data are used for any purpose other than in connection with a definitely Government-related procurement, the United States Government incurs no responsibility or any obligation whatsoever. The fact that the Government may have formulated or in any way supplied the said drawings, specifications, or other data, is not to be regarded by implication, or otherwise as in any manner, as licensing the holder or any other person or corporation; or as conveying any rights or permission to manufacture, use, or sell any patented invention that may in any way be related thereto.

This report is releasable to the National Technical Information Service (NTIS). At NTIS, it will be available to the general public, including foreign nations.

This technical report has been reviewed and is approved for publication.

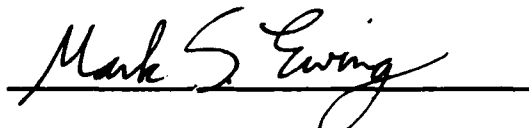


DUANE E. VELEY
Project Engineer
Design & Analysis Methods Group



NELSON D. WOLF, Technical Manager
Design & Analysis Methods Group
Analysis & Optimization Branch

FOR THE COMMANDER



MARK S. EWING, Maj, USAF
Chief, Analysis & Optimization Branch
Structures Division

"If your address has changed, if you wish to be removed from our mailing list, or if the addressee is no longer employed by your organization please notify WRDC/FIBRA, Wright-Patterson AFB OH 45433-6553 to help us maintain a current mailing list".

Copies of this report should not be returned unless return is required by security considerations, contractual obligations, or notice on a specific document.

Unclassified

SECURITY CLASSIFICATION OF THIS PAGE

REPORT DOCUMENTATION PAGE				Form Approved OMB No. 0704-0188	
1a. REPORT SECURITY CLASSIFICATION Unclassified			1b. RESTRICTIVE MARKINGS		
2a. SECURITY CLASSIFICATION AUTHORITY			3. DISTRIBUTION/AVAILABILITY OF REPORT		
2b. DECLASSIFICATION/DOWNGRADING SCHEDULE			Approved for public release; distribution is unlimited		
4. PERFORMING ORGANIZATION REPORT NUMBER(S)			5. MONITORING ORGANIZATION REPORT NUMBER(S) WRDC-TR-90-3012		
6a. NAME OF PERFORMING ORGANIZATION Howard University		6b. OFFICE SYMBOL (If applicable)	7a. NAME OF MONITORING ORGANIZATION Flight Dynamics Lab, WRDC - AFSC		
6c. ADDRESS (City, State, and ZIP Code) Department of Mechanical Engineering Washington, DC 20059			7b. ADDRESS (City, State, and ZIP Code) WRDC/FIBRA Wright Patterson AFB, OH 45433-6553		
8a. NAME OF FUNDING/SPONSORING ORGANIZATION		8b. OFFICE SYMBOL (If applicable)	9. PROCUREMENT INSTRUMENT IDENTIFICATION NUMBER F 33615-88-C-3208		
8c. ADDRESS (City, State, and ZIP Code)			10. SOURCE OF FUNDING NUMBERS		
PROGRAM ELEMENT NO. 62201F		PROJECT NO. 2401	TASK NO. 02	WORK UNIT ACCESSION NO. 88	
11. TITLE (Include Security Classification) Control of Orbiting Large Space Structural Systems with Discrete-Time Observational Data and Random Measurement Noise					
12. PERSONAL AUTHOR(S) Dr. Peter M. Bainum, Prof. Xing Guangqian, and Aprille J. Ericsson					
13a. TYPE OF REPORT Final		13b. TIME COVERED FROM 7/29/88 TO 2/28/89	14. DATE OF REPORT (Year, Month, Day) March 21, 1990		15. PAGE COUNT 73
16. SUPPLEMENTARY NOTATION					
17. COSATI CODES			18. SUBJECT TERMS (Continue on reverse if necessary and identify by block number)		
FIELD	GROUP	SUB-GROUP	Digital control; large space structures; random measurement noise; Kalman filter.		
19. ABSTRACT (Continue on reverse if necessary and identify by block number)					
<p>The objective of this research is to develop practical design procedures that can be used in conjunction with optimal digital controllers and estimators for future orbiting large space structural systems. In practice, observational data used to verify the orientation and shape of large flexible systems will, in general, be collected on a sampled basis (discrete-time data system). Random noise is also included with such observational data. Systems which will be designed to control both the overall orientation as well as the shape of some of the subsystems (such as an antenna mesh form) must function in the discrete-time domain. The aim of this research is to develop methods that can be used to design linear quadratic Gaussian (LQG) controllers/estimators for orbiting large flexible systems. The digital control of an orbiting shallow shell antenna-type system, as well as flexible platform-type systems are examined in this report.</p>					
20. DISTRIBUTION/AVAILABILITY OF ABSTRACT <input type="checkbox"/> UNCLASSIFIED/UNLIMITED <input checked="" type="checkbox"/> SAME AS RPT. <input type="checkbox"/> DTIC USERS			21. ABSTRACT SECURITY CLASSIFICATION Unclassified		
22a. NAME OF RESPONSIBLE INDIVIDUAL Dr. V.B. Venkayya, Mr. Duane Veley			22b. TELEPHONE (Include Area Code) (513) 255-6992		22c. OFFICE SYMBOL WRDC/FIBRA

DD Form 1473, JUN 86

Previous editions are obsolete.

SECURITY CLASSIFICATION OF THIS PAGE

Unclassified

FOREWORD

This final report was prepared by Howard University, Washington DC, for the Analysis and Optimization Branch (FIBR) of the Wright Research and Development Center. The work was performed under Contract F33615-88-C-3208 which was initiated under Project No. 2401 'Structural Mechanics', Task No. 02 'Design and Analysis Methods for Military Flight Vehicle Structures', Work Unit 24010288 'Control of Orbiting Space Structures'. The objective of this contract was to develop methods that can be used to design linear quadratic regulator (LQR) or linear quadratic Gaussian (LQG) controllers/estimators for orbiting space flexible antenna/reflector and platform systems. This report is entitled 'Control of Orbiting Large Space Structural Systems with Discrete Time Observational Data and Random Measurement Noise'. The principal investigator was Dr Peter M. Bainum of the Department of Mechanical Engineering. He was supported by Prof Xing Guanggian and Aprille J. Ericsson. In FIBR Duane Velez was the project monitor while Dr V. B. Venkayya initiated the program and provided overall program direction.

Accession For	
NTIS GRA&I	<input checked="" type="checkbox"/>
DTIC TAB	<input type="checkbox"/>
Unannounced	<input type="checkbox"/>
Justification	
By	
Distribution/	
Availability Codes	
Dist	Avail and/or Special
A-1	



ACKNOWLEDGEMENTS

This research represents the work performed during the period July 29, 1988 to July 28, 1989 on WRDC Contract No. F33615/88C-3208. Special appreciation is extended to Dr. V.B. Venkayya, WRDC/FIBRA Project Engineer who directed this effort.

Thanks are also extended to Capt. Bruce Snyder and Mr. Duane Velez of AFWAL for their helpful comments and constructive criticism. The original background work that provided the initial impetus for this research was initiated with the support of the NASA/Howard University Large Space Structures Institute (LSSI). Appreciation is extended to Dr. Jerrold Housner, NASA Langley LSSI Technical Director and Dr. Taft Broome, Jr., Howard University, LSSI Director.

TABLE OF CONTENTS

SECTION	PAGE
1. INTRODUCTION	1
2. THE OPTIMAL LQG DIGITAL SHAPE AND ORIENTATION CONTROL OF AN ORBITING SHALLOW SPHERICAL SHELL SYSTEM	3
2.1. Introduction	3
2.2. Mathematical Model	3
2.2.1. Dynamical Equations	3
2.2.2. Point Actuator Model	8
2.2.3. Point Sensors and the Observational Model	8
2.2.4. The State Equations of the Shallow Spherical Shell System	10
2.3. The Placement of Actuators	11
2.4. Analysis and Design of the LQG Optimal Regu- lators and Observers for the Shallow Spheri- cal Shell System	13
2.4.1. Model, Problem and Solution	13
2.4.2. The Separation Property and Suboptimal Design	15
2.5. Digital Simulation	19
2.6. Conclusions	25
3. SOME DEFINITIONS OF DEGREE OF CONTROLLABILITY (OBSERVABILITY) FOR DISCRETE-TIME SYSTEMS AND THEIR APPLICATIONS	32
3.1. Introduction	32
3.2. Concept and Physical Meaning of Controlla- bility	32
3.3. Three Candidates for the Definitions of Degree of Controllability and Their General Properties	35
3.4. The Definition of Degree of Observability and Its Physical Meaning	38
3.5. The Degree of Controllability (Observability) for Discrete-Time Invariant Systems	40
3.6. Application	41
3.7. Conclusions	47
4. OPTIMAL DIGITAL CONTROL FOR FREE-FREE ORBITING PLATFORMS	53
4.1. Specific Aims	53
4.2. Justification	53
4.3. Methodology	53
4.4. Expected Results	55
4.5. Why	55

5. CONCLUDING COMMENTS	56
REFERENCES	57
APPENDIX	61

LIST OF FIGURES

FIGURE	CAPTION	PAGE
1.	Orbiting Shallow Spherical Shell System	4
2.	LQG Control of Shallow Spherical Shell Transient Response for Case 2	21
3.	LQG Control of Shallow Spherical Shell Transient Response for Case 4.	22
4.	LQG Control of Shallow Spherical Shell Transient Response for Case 6	23
5.	LQG Control of Shallow Spherical Shell Transient Response for Case 7	24
6.	LQG Control of Shallow Spherical Shell Transient Response for System EC-1 (a)	27
7.	LQG Control of Shallow Spherical Shell Transient Response for System EC-1 (b)	28
8.	LQG Control of Shallow Spherical Shell Transient Response for System EC-2	29
9.	LQG Control of Shallow Spherical Shell Transient Response for System EC-3	30
10.	LQG Control of Shallow Spherical Shell Transient Response for System EC-4	31
11.	LQG Control of Shallow Spherical Shell Transient Response for Case 2 - a (six actuators)	48
12.	LQG Control of Shallow Spherical Shell Transient Response for Case 2 - b (six actuators)	49
13.	LQG Control of Shallow Spherical Shell Transient Response for Case 7 - a (six actuators)	50
14.	LQG Control of Shallow Spherical Shell Transient Response for Case 7 - b (six actuators)	51
15.	The First Modal Amplitude for Case 2 and Case 7 ...	52

LIST OF TABLES

TABLE	CAPTION	PAGE
1.	Frequencies and Coefficients of Shape Function	7
2.	The Degree of Controllability for Different Locations of Actuators on the Shallow Spherical Shell	12
3.	The Relationship Between the Position of the Regu- lator Poles and Weighting Matrix R	17
4.	The Max. and Min. Moduli of the Eigenvalues of \tilde{A}^* vs. Parameters μ_R , μ_Q for Case 6 and Case 7 ($R = \mu_R I$, $Q = \mu_Q I$)	18
5.	The Parameters of the System EC1 - EC4	26
6.	The Actuator Locations (ξ , β) and Force Directions (f_x , f_y , f_z)	43
7.	The Degree of Controllability for the Different Cases	46

SUMMARY

The objective of this research is to develop practical design procedures that can be used in conjunction with optimal digital controllers and estimators for future orbiting large space structural systems. In practice, observational data used to verify the orientation and shape of large flexible systems will, in general, be collected on a sampled basis (discrete-time data system). Random noise is also included with such observational data. Systems which will be designed to control both the overall orientation as well as the shape of some of the subsystems (such as an antenna mesh form) must function in the discrete-time domain. The aim of this research is to develop methods that can be used to design linear quadratic regulator (LQR) or linear quadratic Gaussian (LQG) controllers/estimators for orbiting large flexible systems. The digital control of an orbiting shallow shell antenna-type system, as well as flexible platform-type systems are examined in this report.

1. INTRODUCTION

The purpose of this research is to study and develop the practical methods of designing LQR and LQG digital controllers and estimators for orbiting large space flexible structural systems.

A number of investigators [1-6] have considered the problem of developing optimal control laws for large flexible orbiting systems under the assumption that the state vector information would be observed directly or that the state information could be estimated on a continuous basis. In practice, however, the observational data, in general, will most probably be collected on a sampled basis i.e. a discrete-time data system. [7-10] Sometimes the random noise which is included in the observational data cannot be neglected. In this case, the observational data must be treated as observational data with random measurement noise. Therefore, it appears useful and timely to study the control problem of orbiting large space structural systems with discrete-time observational data and random measurement noise. [11, 12]

The analysis and design of LQR digital controllers and LQG digital controllers and estimators have been finished for a hypothetical thin free-free long beam in orbit. The concepts of the degree of controllability (observability) which is a function of the controllability (observability) matrix [13-16] have been applied to solve the problem of actuator and sensor placement. The closed-loop dynamics of the LQR and LQG control system for a long, slender orbiting flexible beam have been simulated. The design of the digital controllers and estimators has been certified by simulation.

The aim of this reported research, for the period July 1988 - July 1989, is to develop methods that can be used to design linear quadratic regulator (LQR) or linear quadratic Gaussian (LQG) controllers/estimators for orbiting space flexible antenna/reflector and platform systems. The specific tasks reported are as follows:

(1) The analysis and design of the LQR and LQG digital controllers and estimators for large space flexible shallow spherical shell systems representative of orbiting reflector/antenna systems. A paper based on this task has been accepted for presentation at the 40th International Astronautical Congress and is the basis for Chapter 2 of this report.

(2) The development of three definitions of the degree of controllability (observability) which are based on the scalar measure of the controllability (observability) matrix for discrete-time systems. Their general properties, together with the simple physical and geometrical interpretations for the fuel optimal control problem are shown. The applications of these definitions for the actuator placement problem of the orbiting shallow spherical shell system are illustrated for seven sample cases. A paper based on this task has been presented at the 12th Biennial Conference on Mechanical Vibration and Noise and is the nucleus for Chapter 3 of this report.

(3) Modelling of large flexible orbiting platform control systems and the analysis and design of LQR digital controllers for large flexible orbiting platform systems. This is in progress and will be the basis of a Master's thesis, currently under preparation. A brief summary of this task is presented in Chapter 4 of this report. It is intended that the Master's thesis will also be published as a supplement to this volume.

(4) Finally, Chapter 5 will summarize some concluding statements and follow-on plans for the continuation of this general area of research along the lines of our recent proposal^[17] to WRDC.

2. THE OPTIMAL LQG DIGITAL SHAPE AND ORIENTATION CONTROL OF AN ORBITING SHALLOW SPHERICAL SHELL SYSTEM

2.1 Introduction

Future proposed space missions would involve large inherently flexible systems for use in communications, radiometry, and in electronic orbital based mail systems. The use of very large shallow dish type structures to be employed as receivers/reflectors for these missions has been suggested. In order to satisfy mission requirements control of the shape as well as the overall orientation will often be required. The proposed paper is devoted to a study of the LQG digital optimal control of the shape and orientation for an orbiting shallow spherical shell system.

The dynamical system equations and deterministic control of the three-dimensional shallow spherical shell in orbit, in which the yaw, roll and pitch attitude angles of the undeformed shell and six flexible modal parameters are modeled, have been studied.[1, 18-19] In this paper the LQG digital optimal control technique will be applied to the shape and attitude control of shallow spherical shell systems. In order to realize estimation and control, the mathematical models for the actuators and sensors are developed, in which up to 12 jet actuators are used for control of the attitude and shape of the shell. For observation, two sun sensors, two earth horizon sensors and six displacement sensors are assumed to be used for measuring the attitude and displacement of the deformed shell.

As for the suboptimal digital LQG problem[12] we are not only interested in the separate design of both the controller and estimator, but more interested in determining the influence of the different combinations of the controller and observer pole locations on the estimate and control process and the best combination of controller and observer pole locations.

In addition, the problem of actuator placement is discussed by means of the concept of the degree of controllability.[20] The best arrangement of the locations for the actuators will be discussed.

Finally, the simulations certify the analysis and design of the digital optimal controllers and estimations.

2.2 Mathematical Model

2.2.1 Dynamical Equations

The mathematical model of an isotropic shallow flexible spherical shell in orbit was developed in references [1, 18-19]. The main assumption is that the shell's elastic displacements were principally in the transverse direction (parallel to the symmetry axis) and were small as compared with the other characteristic dimensions of the shell. The assumption of shallowness further insures that the ratio of the displacement of the shell's apex point above its base plane (H) is small as compared with the radius in the base plane, l , (Figure 1).

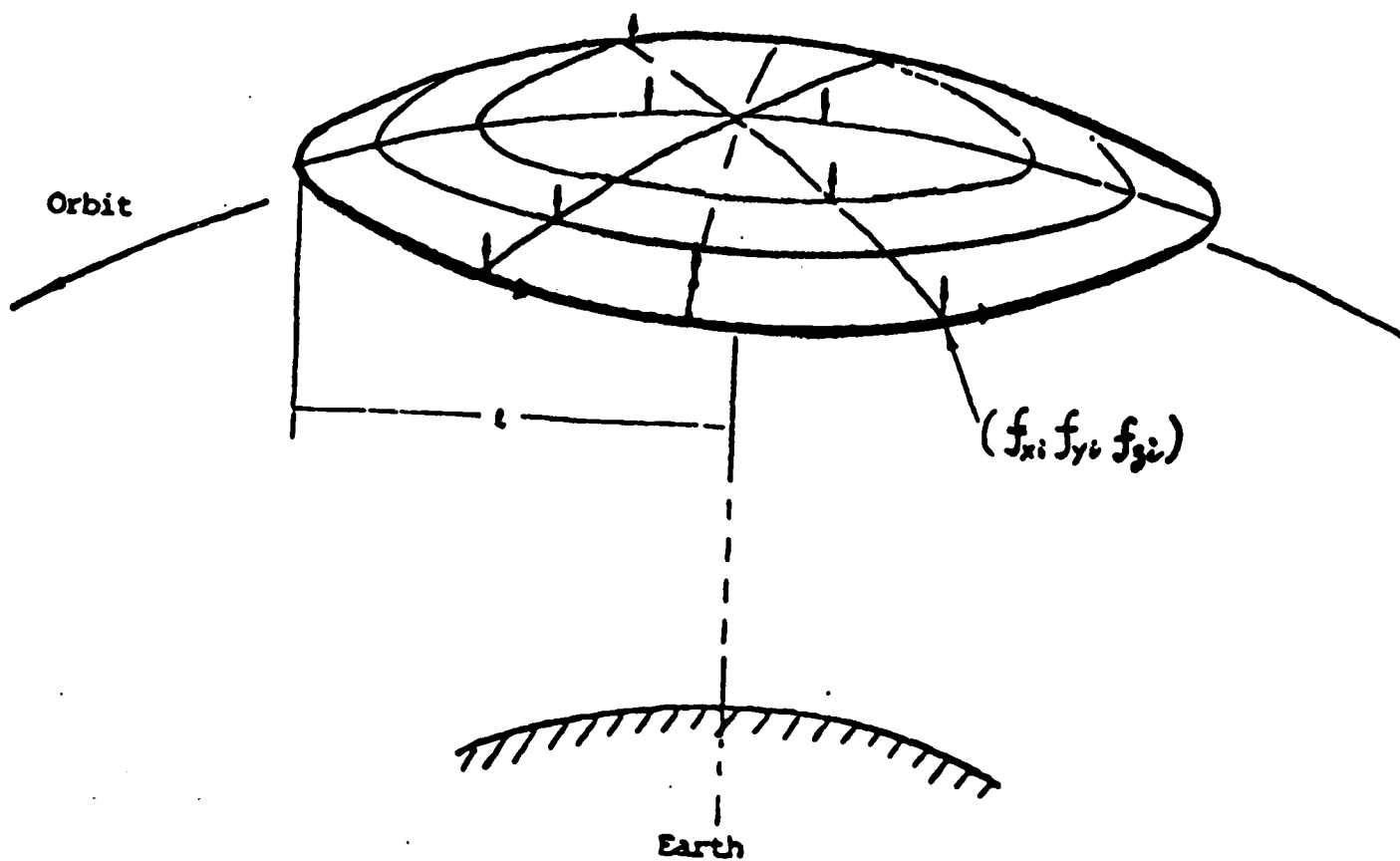


Figure 1. Orbiting Shallow Spherical Shell System

The resulting linearized equations of motion for the rigid rotational and generic elastic modes were developed as:

$$\ddot{\Psi} - \mu_1 \dot{\Psi} - (1 + \mu_1) \dot{\phi} = C_x / J_x^{(0)} \omega_c^2$$

$$\ddot{\phi} + 4\mu_3 \dot{\phi} + (1 - \mu_3) \dot{\Psi} = C_z / J_z^{(0)} \omega_c^2$$

$$\ddot{\theta} - 3\mu_2 \dot{\theta} - (2l / J_y^{(0)}) \sum_{n=1}^6 I_1^{(n)} \dot{\epsilon}_n = C_y / J_y^{(0)} \omega_c^2 \quad (1)$$

$$\ddot{\epsilon}_i + (\Omega_i^2 - 3) \epsilon_i + (2I_1^{(1)} / M_i l) \dot{\theta} = 3I_1^{(1)} / M_i l + E_i / M_i l \omega_c^2 \quad (i = 1, 2, \dots, 6)$$

where

$$\tau = \omega_c t, \quad \epsilon_i = q_i(t) / l \quad (i = 1, 2, \dots, 6)$$

The derivative in Equation (1) is with respect to τ .

Ψ, ϕ, θ yaw, roll and pitch angles, respectively, between the undeformed axes of the shallow spherical shell and the axes of the orbiting local vertical/local horizontal system

$q_i(t)$ modal amplitude of the i th generic mode

ω_c orbital angular rate, constant for assumed circular orbit

l characteristic length (the base radius)

M_i the i th modal mass

$J_x^{(0)}, J_y^{(0)}, J_z^{(0)}$ principal moments of inertia of the undeformed shell

C_x, C_y, C_z the components of external torques

X_c coordinate of differential area on the surface above the base plane

μ_1, μ_2, μ_3 $(J_z^{(0)} - J_y^{(0)}) / J_x^{(0)}, (J_x^{(0)} - J_z^{(0)}) / J_y^{(0)},$
 $(J_y^{(0)} - J_x^{(0)}) / J_z^{(0)},$ respectively

$I_1^{(1)}$ $\int X_c \phi_x^{(1)} dv$

ϕ_x transverse component of the i th modal shape function

ω_n natural frequency of n th mode

Ω_n ω_n/ω_c

The frequencies, ω , of the spherical shell are evaluated using the following identities, as presented by Johnson and Reissner.[21]

$$\omega_{pj}^2 = \left(\frac{D}{h\rho l^4}\right) \mu_{pj}^4 + \omega_\infty^2 \quad (2)$$

where

$D = Eh^3/12(1-\nu^2)$, ending stiffness factor

$\omega_\infty^2 = E/\rho R^2$

ν = Poisson's ratio

ρ = density of shell material

E = modulus of elasticity

h = wall thickness of the shell

l = the base radius of the shell

R = radius of curvature of the shell

The μ_{pj} are calculated from

$$\frac{\mu_{pj}}{2} \left\{ \frac{J_p(\mu_{pj})}{J_{p+1}(\mu_{pj})} + \frac{I_p(\mu_{pj})}{I_{p+1}(\mu_{pj})} \right\} = 1-\nu \text{ for } p=0,1 \quad (3)$$

For the sample calculations in this paper, we will consider only such values of μ_{pj} ($j = 1, 2, 3$) for the cases where $p = 0, 1$.

The mode shapes of the transverse vibrations of a shallow spherical shell with a completely free edge are given by:[21, 22]

$$\phi_x^{(n)} = A_{pj} \left\{ \frac{l^{p+4}}{RD\mu_{pj}^4} C_{pj} \xi^p + J_p(\mu_{pj}, \xi) + D_{pj}(\mu_{pj}, \xi) \right\} \cos p(\theta + \theta_0) \quad (4)$$

where p the number of nodal diameters (meridians)

j the number of nodal circles

For the following proposal numerical values considered: $H = 1\text{m}$; $l = 100\text{m}$; $h = 0.01\text{m}$; $\nu = 1/3$; $R = 5000\text{m}$; $\rho = 31.8309 \text{ kg/m}^3$; $E = 0.840466 \times 10^9 \text{ Newton/m}^2$; the frequencies and the shape function coefficients are shown in Table 1. ($C_{pj} = 0$; $p = 0, 1$; $j = 1, 2, 3$)

TABLE 1. FREQUENCIES AND COEFFICIENTS OF
SHAPE FUNCTION

$n(p,j)$	p	j	μ_{pj}^2	ω_n (rad./s)	A_{pj}	D_{pj}
1	0	1	9.076	1.02778	2.1979	-0.8381×10^{-1}
2	0	2	38.507	1.02946	3.1389	0.3119×10^{-2}
3	0	3	87.82	1.03692	3.8468	-0.12787×10^{-3}
4	1	1	20.52	1.02163	3.8359	-0.1901×10^{-1}
5	1	2	59.86	1.03198	4.9627	0.7045×10^{-3}
6	1	3	119.00	1.04459	5.8752	-0.2845×10^{-4}

2.2.2 Point Actuator Model

The point actuators are modelled as follows. Let the i th actuator be located at (l_{x1}, l_{y1}, l_{z1}) and the force component of the i th actuator be $(f_{x1}, f_{y1}, f_{z1})/|f_1|$. The torques provided by the α actuators are as follows:

$$C = \begin{pmatrix} C_x \\ C_y \\ C_z \end{pmatrix} = \sum_i^{\alpha} \begin{pmatrix} 0 & -l_{z1} & l_{y1} \\ l_{z1} & 0 & -l_{x1} \\ -l_{y1} & l_{x1} & 0 \end{pmatrix} \begin{pmatrix} f_{x1} \\ f_{y1} \\ f_{z1} \end{pmatrix} |f_1| \quad (5)$$

The corresponding generic force in the n th mode,

$$E_n = \int \phi^{(n)} \left(\sum_i^{\alpha} f_{i1}/M \right) \delta(x-x_1, y-y_1, z-z_1) dm \quad (6)$$

For the shallow spherical shell it is assumed that the major elastic displacement occurs in a direction normal to the base (y, z) plane, i.e., $\phi^{(n)} = \phi_x^{(n)}(\xi, \beta) \hat{i}$. The control forces provided by the α actuators are

$$f = \sum_i^{\alpha} f_{i1} = \sum_i^{\alpha} (f_{x1} \hat{i} + f_{y1} \hat{j} + f_{z1} \hat{k}) |f_1| \quad (7)$$

Substituting (7) into Equation (6), we have

$$E_n = \sum_i^{\alpha} \phi_x^{(n)}(\xi_1, \beta_1) f_{x1} |f_1| \quad (8)$$

2.2.3 Point Sensors and the Observational Model

In order to describe the geometric relationship between the orientation and reference systems, it is necessary to define the following coordinate reference systems:

$\{\hat{i}_1, \hat{j}_1, \hat{k}_1, E\}$ Earth inertial coordinate system, its center is the center of Earth, \hat{i}_1 axis points to the spring equinox.

$\{\hat{i}_0, \hat{j}_0, \hat{k}_0, 0\}$ Orbital reference system, its center is the mass center of the undeformed shell, the \hat{i}_0 is along the outward local vertical from the center of the Earth.

$\{\hat{i}, \hat{j}, \hat{k}, 0\}$ The body reference system of the undeformed shell, i.e., the principal axes system of the undeformed shell.

The relationships between the coordinate reference systems are as follows:

$$\begin{pmatrix} \hat{i}_0 \\ \hat{j}_0 \\ \hat{k}_0 \end{pmatrix} = A_{01}(\omega_p + f_e, i, \Omega) \begin{pmatrix} \hat{i}_1 \\ \hat{j}_1 \\ \hat{k}_1 \end{pmatrix} \quad (9)$$

where ω_p is the argument of perigee, f_e is the true anomaly angle, i is the orbital inclination, and Ω is the right ascension of the ascending node line.

$$\begin{pmatrix} \hat{i} \\ \hat{j} \\ \hat{k} \end{pmatrix} = A_{b0}(\phi, \theta, \psi) \begin{pmatrix} \hat{i}_0 \\ \hat{j}_0 \\ \hat{k}_0 \end{pmatrix} \quad (10)$$

where

$$A_{b0} = \begin{pmatrix} \cos\phi\cos\theta & \sin\phi\cos\psi + \cos\phi\sin\theta\sin\psi & \sin\phi\sin\psi - \cos\phi\sin\theta\cos\psi \\ -\sin\phi\cos\theta & \cos\phi\cos\psi - \sin\phi\sin\theta\sin\psi & \cos\phi\sin\psi + \sin\phi\sin\theta\cos\psi \\ \sin\theta & -\cos\theta\sin\psi & \cos\theta\cos\psi \end{pmatrix}$$

It is assumed that two earth horizon sensors are used for measuring the angle, θ_{e2} , between the axis \hat{j} and \hat{i}_0 , and the angle, θ_{e3} , between the axis \hat{k} and \hat{i}_0 . The observational geometrical relationships are as follows:

$$\cos\theta_{e2} = \hat{j} \cdot \hat{i}_0 = -\sin\phi \cos\theta \quad (11)$$

$$\cos\theta_{e3} = \hat{k} \cdot \hat{i}_0 = \sin\theta \quad (12)$$

It is assumed that two sun sensors are used for measuring the angle, θ_{s2} , between the axis \hat{j} and the direction vector of the sun, \hat{s} , and the angle, θ_{s3} , between the axis \hat{k} and \hat{s} . The observational geometrical relationships are as follows:

$$\begin{aligned} \cos\theta_{s2} = \hat{j}_0 \cdot \hat{s} = & -\sin\phi\cos\theta(\hat{i}_0 \cdot \hat{s}) + (\cos\phi\cos\psi - \sin\phi\sin\theta\sin\psi)(\hat{j}_0 \cdot \hat{s}) \\ & + (\cos\phi\sin\psi + \sin\phi\sin\theta\cos\psi)(\hat{k}_0 \cdot \hat{s}) \end{aligned} \quad (13)$$

$$\cos\theta_{s3} = \hat{k} \cdot \hat{s} = \sin\theta(\hat{i}_0 \cdot \hat{s}) - \cos\theta\sin\psi(\hat{j}_0 \cdot \hat{s}) + \cos\theta\cos\psi(\hat{k}_0 \cdot \hat{s}) \quad (14)$$

It is assumed that γ displacement sensors are used to measure the shell's transverse displacement parallel to the x axis, i.e.,

$$\begin{aligned} g_1 &= C_f \bar{U}(\xi_1, \beta_1; t) \cdot \hat{i} \\ &= C_f \sum_j \phi_x^{(j)}(\xi_1, \beta_1) q_j(t) \\ &= C_f \ell \sum_j \phi_x^{(j)}(\xi_1, \beta_1) \varepsilon_j(t) \end{aligned} \quad (15)$$

(1 = 1, 2, ..., γ)

where

$\bar{U}(\xi_1, \beta_1; t)$ displacement vector of the shell at (ξ_1, β_1)

C_f coefficient relating the displacement to the output voltage

l the base radius of the shell

The linearized version of Equations 11-14 and Equation 15 are combined into the observation equation for the shell system as follows:

$$Y = Hx \quad (16)$$

where

$$Y = \begin{bmatrix} \cos \theta_{e2} \\ \cos \theta_{e3} \\ \cos \theta_{s2} - (\hat{j}_0 \cdot \hat{s}) \\ \cos \theta_{s3} - (\hat{k}_0 \cdot \hat{s}) \\ g_1 \\ g_2 \\ \vdots \\ g_Y \end{bmatrix}$$

$$H = \begin{bmatrix} \begin{pmatrix} 0 & -1 & 0 \\ 0 & 0 & 1 \\ (\hat{k}_0 \cdot \hat{s}) - (\hat{i}_0 \cdot \hat{s}) & 0 \\ -(\hat{j}_0 \cdot \hat{s}) & 0 & (\hat{i}_0 \cdot \hat{s}) \end{pmatrix}_{4 \times 3} & \begin{pmatrix} 0 \end{pmatrix}_{4 \times 6} & \begin{pmatrix} 0 \end{pmatrix}_{(4+Y) \times 9} \\ \begin{pmatrix} 0 \end{pmatrix}_{Y \times 3} & C_f l \begin{bmatrix} \begin{matrix} (1) & (2) & (6) \\ (\phi_x(\xi_1, \beta_1) \phi_x(\xi_1, \beta_1) \dots \phi_x(\xi_1, \beta_1) \end{matrix} \\ \begin{matrix} (1) & (2) & (6) \\ (\phi_x(\xi_2, \beta_2) \phi_x(\xi_2, \beta_2) \dots \phi_x(\xi_2, \beta_2) \end{matrix} \\ \dots \\ \begin{matrix} (1) & (2) & (6) \\ (\phi_x(\xi_Y, \beta_Y) \phi_x(\xi_Y, \beta_Y) \dots \phi_x(\xi_Y, \beta_Y) \end{matrix} \end{bmatrix}_{Y \times 6} & \begin{pmatrix} 0 \end{pmatrix}_{(4+Y) \times 19} \end{bmatrix}$$

2.2.4 The State Equations of the Shallow Spherical Shell System

Considering Equations 5 and 8, Equation 1 can be written in the state vector form:

$$\dot{x} = Ax + Bu \quad (17)$$

where

$$\begin{aligned} x &= (\psi, \phi, \theta, \epsilon_1, \epsilon_2, \epsilon_3, \dots, \epsilon_6, \dot{\psi}, \dot{\phi}, \dot{\theta}, \dot{\epsilon}_1, \dot{\epsilon}_2, \dots, \dot{\epsilon}_6)^T \\ u &= (|r_1|, |r_2|, \dots, |r_n|)^T \end{aligned}$$

$$A = \begin{pmatrix} 0 & I \\ -\bar{A} & D \end{pmatrix} \quad B = \begin{pmatrix} 0 \\ \bar{B} \end{pmatrix}$$

$$\bar{A} = \begin{pmatrix} \bar{a}_{11} & & & & & \\ & \bar{a}_{22} & & & & \\ & & \ddots & & & \\ & & & \ddots & & \\ & & & & \ddots & \\ & & & & & \bar{a}_{99} \end{pmatrix} \quad D = \begin{pmatrix} d_{12} & & & & & \\ d_{21} & & & & & \\ & d_{34} & d_{35} & d_{36} & & \\ & & d_{43} & & & \\ & & d_{53} & & & \\ & & d_{63} & & & \end{pmatrix}$$

The state Equation (17) can be discretized as follows

$$x(k+1) = \Phi(\Delta T)x(k) + \Gamma(\Delta T)u(k) \quad (18)$$

where

$$\Phi(\Delta T) = e^{A\Delta T} \quad ; \quad \Delta T \text{ sampling time}$$

$$\Gamma(\Delta T) = \int_0^{\Delta T} \Phi(\Delta T-t) B \, dt$$

The discretized observation equation is as follows

$$Y(k) = Hx(k) \quad (19)$$

2.3. The Placement of Actuators

The concept of the degree of controllability has been used for determining the placement of actuators on the shell. The detailed results of this study are described in reference [20]. In this paper we only list part of the main results in Table 2.

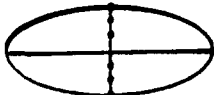





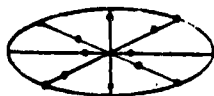
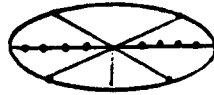
The degree of controllability is the scalar measure of system controllability and its reciprocal indicates the control effort of the system. The degree of controllability, μ_1 , in Table 2, is defined as follows:

$$\mu_1 = \lambda_{\min}(W_c) \quad (20)$$

where

$$\begin{aligned} W_c &= P_c P_c^T \\ P_c &= (\Gamma \quad \Phi\Gamma \quad \Phi^2\Gamma \quad \dots \quad \Phi^{n-1}\Gamma) \end{aligned}$$

TABLE 2. THE DEGREE OF CONTROLLABILITY FOR DIFFERENT LOCATIONS OF ACTUATORS ON THE SHALLOW SPHERICAL SHELL

Case	No. Actuators	Locations of Actuators	Degree of Controllability, μ_1
1	6		0.0
2	6		0.13875×10^{-12}
3	6		0.14332×10^{-10}
4	6		0.14332×10^{-10}
5	12		0.28673×10^{-10}
6	12		0.85391×10^{-12}
7	12		0.45342×10^{-10}
8	12		0.45349×10^{-10}

The values of the degree of controllability for each case are listed in Table 2. The reason why the degree of controllability for Case 1 is zero is that all the actuators are located along the meridional nodal line of one of the fundamental shell vibrational modes. The reason why the degree of controllability for Case 6 is so low is that the actuators are all located on the same nodal circle ($\xi = \text{const.}$).

It is assumed that the thrusters which are located at the shell's edge have two jet directions: (i) tangent to the shell's edge and (ii) normal to the shell surface. Each of the other thrusters has only one jet direction - normal to the shell's surface.

If the number of actuators is limited to 12, the arrangement of actuators as in Case 7 or Case 8 is suggested.

2.4 Analysis and Design of the LQG Optimal Regulators and Observers for the Shallow Spherical Shell System

The dynamic equations and observational equations of the shallow spherical shell system, as a deterministic model, have been developed in the previous section. They are Equations 18 and 19. In fact, dynamic systems are driven not only by our own control input, but also by disturbances which we can neither control nor model deterministically. Sensors generally do not provide exact readings of desired quantities, but introduce their own system dynamics and distortions as well. Furthermore, these devices are also always noise corrupted. In order to solve these difficulties, the theory and method of the LQG problem (design of the optimal stochastic controller for a problem described in terms of linear system models, quadratic cost criteria, and Gaussian noise models) are effective. In this section the LQG theory is applied to the design of sub-optimal regulators and estimators for the shallow spherical shell system.

2.4.1 Model, Problem and Solution^[12]

Let a system be adequately described by the n-dimensional state difference equations:

$$x(k+1) = \Phi x(k) + \Gamma u(k) + w(k) \quad (21)$$

where the p-dimensional $u(k)$ is the control input to be applied and $w(k)$ is the n-dimensional zero-mean white Gaussian discrete-time noise with

$$E\{w(i) w^T(j)\} = Q \delta_{ij} \quad (22)$$

and assumed to be independent of the initial state condition. The initial $x(0)$ is modeled as a Gaussian random vector with mean $\bar{x}(0)$,

and covariance, P_0 . Available from the system are m -dimensional sampled-data measurements of the form

$$Y(k) = Hx(k) + v(k) \quad (23)$$

where $v(k)$ is the m -dimensional zero-mean white Gaussian discrete-time noise with

$$E\{v(i)v^T(j)\} = R\delta_{ij} \quad (24)$$

and assumed independent of both $x(0)$ and $w(\cdot)$.

The system of Equations 21-24 describes a time-invariant system with stationary noise. If the system model is stabilizable and detectable, there will be constant gain for both the controller and observer dynamics. The stochastic optimal control, u , will minimize a quadratic cost function of the form:

$$J = E\left\{\frac{1}{2} \sum_{i=1}^{\infty} [x^T(i)\hat{Q}x(i) + u^T(i)\hat{R}u(i)]\right\} \quad (25)$$

The LQG solution for the time-invariant system with the stationary random noise model is [11, 12]

$$u(k) = -G^*\hat{x}(k) \quad (26)$$

$$G^* = (\hat{R} + r^T\bar{P}r)^{-1}r^t\bar{P}\phi \quad (27)$$

where the \bar{P} satisfies the algebraic Riccati equation

$$\bar{P} = (\phi - rG^*)^T\bar{P}(\phi - rG^*) + G^{*T}\hat{R}G^* + \hat{Q} \quad (28)$$

The state estimate, $\hat{x}(k)$, is given by

$$\hat{x}(k) = \hat{x}(k/k-1) + \bar{K}(Y(k) - H\hat{x}(k/k-1)) \quad (29)$$

where

$$\hat{x}(k/k-1) = \phi\hat{x}(k-1) + r u(k-1) \quad (30)$$

and

$$\bar{K} = \bar{P}_e H^T (H \bar{P}_e H^T + R)^{-1} \quad (31)$$

The covariance of the state estimate, P_e , satisfies the algebraic Riccati equation

$$\bar{P}_e = (\phi - \bar{K}^* H) \bar{P}_e (\phi - \bar{K}^* H)^T + \phi \bar{K} \bar{K}^T \phi^T + Q \quad (32)$$

where

$$\bar{K}^* = \phi \bar{K} \quad (33)$$

2.4.2 The Separation Property and Suboptimal Design

It is wise to seek the possibility of a separate determination of the optimal state estimate and the optimal controller. Due to computational delay, what is often considered for implementation is not the control law given by Equation 26, but a suboptimal control

$$u(k) = -G^* \hat{x}(k/k-1) \quad (34)$$

where

$$\hat{x}(k+1/k) = \phi \hat{x}(k/k-1) + \Gamma u(k) + \phi \bar{K} (Y(k) - H \hat{x}(k/k-1))$$

Define the error of the predicted estimate of the state as,

$$\Delta x(k/k-1) = x(k) - \hat{x}(k/k-1) \quad (35)$$

the $x(k+1)$ and $\Delta x(k+1/k)$ may be combined into a simple system described by the state equations [23]

$$\begin{pmatrix} x(k+1) \\ \Delta x(k+1/k) \end{pmatrix} = \begin{pmatrix} \phi - \Gamma G^* & \Gamma G^* \\ 0 & \phi - \bar{K}^* H \end{pmatrix} \begin{pmatrix} x(k) \\ \Delta x(k/k-1) \end{pmatrix} + \begin{pmatrix} I & 0 \\ I & -\phi \bar{K} \end{pmatrix} \begin{pmatrix} w(k) \\ v(k) \end{pmatrix} \quad (36)$$

where

$$\bar{K}^* = \phi \bar{K}$$

The output equation of the complete system has the form

$$Y(k) = (H \ ; \ 0) \begin{pmatrix} x(k) \\ \Delta x(k/k-1) \end{pmatrix} + v(k) \quad (37)$$

From Equation 36, the LQG suboptimal control dynamics also consist of two parts: the dynamics of the plant with a feedback controller and the dynamics of the estimator feedback loop. The matrix describing the dynamics of the closed loop controller is

$$A^* = \phi - \Gamma G^* \quad (38)$$

whereas the analogous matrix for the closed-loop estimator is

$$\hat{A}^* = \phi - \bar{K}^* H \quad (39)$$

where

$$\bar{K}^* = \phi \bar{K}$$

The eigenvalues of A^* and \hat{A}^* are independent of each other. In the synthesis of the control loop it is, therefore, possible to arrange the poles of the estimators and controllers separately. Therefore, the eigenvalues of the closed-loop system simply consist of the regulator poles and observer poles, i.e., the eigenvalues of A^* and \hat{A}^* , respectively. It is well known that, in the time-invariant system case, if and only if the open-loop system model is both stabilizable with respect to $u(k)$ and detectable with respect to

$y(k)$, there do exist gains G^* and \hat{K}^* that can provide asymptotic closed-loop stability. Furthermore, under the stronger assumptions of complete controllability and complete observability, we can place both the regulator and observer poles arbitrarily (within the restriction of the complex conjugate pairs).

It is assumed for system (21), (23) that the pair (Φ, Γ) is either completely controllable or stabilizable by state feedback, and the pair (Φ, H) is either completely observable or detectable, then the gain matrix of the controller, G^* , and the gain matrix of observer, \hat{K}^* , may be obtained from Equations 27, 28 and 31, 32, 33, respectively. They are functions of the weighting matrices \hat{R} , \hat{Q} and the observational noise variance, R , and the system noise variance, Q , respectively. Therefore, the eigenvalues of the closed-loop controller A^* will be changed by means of the changes of the weighting matrices, \hat{R} , \hat{Q} ; and, similarly, the eigenvalues of the closed-loop observer \hat{A}^* are also changed with the variation of the matrices, R and Q .

Let

$$\hat{Q} = H^T H, \quad \hat{R} = \mu_C I_0$$

$$Q = \mu_Q I_0, \quad R = \mu_R I_0$$

In order to find the appropriate arrangement of the controller and observer poles, it is necessary to study the loci of the A^* eigenvalues and the \hat{A}^* eigenvalues with μ_C or μ_R , μ_Q . The loci of the maximum and minimum moduli of the eigenvalues of A^* for the systems of Case 6 and Case 7 in Table 2 are listed in Table 3.

The maximum and minimum moduli of the eigenvalues for \hat{A}^* vs. the different parameters, μ_R and μ_Q , are listed in Table 4.

It is assumed that the covariances of the measurement noise and the system (plant) noise are $R_S = 10^{-6} I_0$ and $Q_S = 10^{-10}$, respectively. Based on this data and Tables 2-4, we can arrange the position of the controller and observer poles. The procedures are as follows:

(1) Placement of actuators: Based on the calculation of the degree of controllability for different arrangement of actuators, to determine the best placement of the actuators. As shown in Table 2, if the number of actuators is 12, the better placements are indicated in Cases 7 and 8. Case 7 is proposed to be simulated for the design of the controller and observer.

TABLE 3. THE RELATIONSHIP BETWEEN THE POSITION OF THE REGULATOR
POLES AND WEIGHTING MATRIX \hat{R}

$\hat{R} = \mu_C I_0$ μ_C	Case 6		Case 7	
	Moduli of A^* Eigenvalues Min.	Max.	Moduli of A^* Eigenvalues Min.	Max.
10^{-16}	0.30717×10^{-7}	0.99997	0.30334×10^{-7}	0.99998
10^{-14}	0.42290×10^{-7}	0.99969	0.33982×10^{-7}	0.99982
10^{-12}	0.11522×10^{-5}	0.99696	0.39831×10^{-6}	0.99826
10^{-10}	0.11217×10^{-3}	0.97817	0.36832×10^{-4}	0.98271
10^{-8}	0.11718×10^{-1}	0.97818	0.37316×10^{-2}	0.83858
10^{-6}	0.48849	0.97865	0.35403	0.93776
10^{-4}	0.90319	0.98828	0.86382	0.98745
10^{-2}	0.96867	0.99848	0.96763	0.99806
1	0.98768	0.99984	0.98809	0.99981
10^2	0.99037	0.99998	0.99038	0.99997
10^4	0.99042	0.99999	0.99042	0.99999
10^6	0.99042	0.99999	0.99042	0.99999

TABLE 4. THE MAX. AND MIN. MODULI OF THE EIGENVALUES OF \hat{A}^* VS. PARAMETERS μR , μQ FOR CASE 6 AND CASE 7
($R = \mu R I$, $Q = \mu Q I$)

μQ	10^{-2}	10^{-4}	10^{-6}	10^{-8}	10^{-10}	10^{-12}	10^{-14}	10^{-16}	10^{-2}	10^{-4}	10^{-6}	10^{-8}	10^{-10}	10^{-12}	10^{-14}	10^{-16}	μR
10^{-2}	0.422402x10 ⁻² 0.99440	0.42240x10 ⁻² 0.99440	0.42240x10 ⁻² 0.99440	0.42240x10 ⁻² 0.99440	0.42240x10 ⁻² 0.99440	0.42240x10 ⁻² 0.99440	0.42240x10 ⁻² 0.99440	0.42240x10 ⁻² 0.99440	0.41142x10 ⁻² 0.99440	0.41142x10 ⁻² 0.99440	0.41142x10 ⁻² 0.99440	0.41142x10 ⁻² 0.99440	0.41142x10 ⁻² 0.99440	0.41142x10 ⁻² 0.99440	0.41142x10 ⁻² 0.99440	0.41142x10 ⁻² 0.99440	0.32581 0.99440
10^{-4}	0.42240x10 ⁻² 0.99440	0.42240x10 ⁻² 0.99440	0.42240x10 ⁻² 0.99440	0.42240x10 ⁻² 0.99440	0.42240x10 ⁻² 0.99440	0.42240x10 ⁻² 0.99440	0.42240x10 ⁻² 0.99440	0.42240x10 ⁻² 0.99440	0.41142x10 ⁻² 0.99440	0.41142x10 ⁻² 0.99440	0.41142x10 ⁻² 0.99440	0.41142x10 ⁻² 0.99440	0.41142x10 ⁻² 0.99440	0.41142x10 ⁻² 0.99440	0.41142x10 ⁻² 0.99440	0.41142x10 ⁻² 0.99440	0.52903 0.99450
10^{-6}	0.422430x10 ⁻² 0.99440	0.42240x10 ⁻² 0.99440	0.42240x10 ⁻² 0.99440	0.42240x10 ⁻² 0.99440	0.42240x10 ⁻² 0.99440	0.42240x10 ⁻² 0.99440	0.42240x10 ⁻² 0.99440	0.42240x10 ⁻² 0.99440	0.41142x10 ⁻² 0.99440	0.41142x10 ⁻² 0.99440	0.41142x10 ⁻² 0.99440	0.41142x10 ⁻² 0.99440	0.41142x10 ⁻² 0.99440	0.41142x10 ⁻² 0.99440	0.41142x10 ⁻² 0.99440	0.41142x10 ⁻² 0.99440	0.74399 0.99450
10^{-8}	0.42240x10 ⁻² 0.99440	0.42229x10 ⁻² 0.99440	0.42229x10 ⁻² 0.99440	0.42229x10 ⁻² 0.99440	0.42229x10 ⁻² 0.99440	0.42229x10 ⁻² 0.99440	0.42229x10 ⁻² 0.99440	0.42229x10 ⁻² 0.99440	0.41142x10 ⁻² 0.99440	0.41142x10 ⁻² 0.99440	0.41142x10 ⁻² 0.99440	0.41142x10 ⁻² 0.99440	0.41142x10 ⁻² 0.99440	0.41142x10 ⁻² 0.99440	0.41142x10 ⁻² 0.99440	0.41142x10 ⁻² 0.99440	0.90492 0.99742
10^{-10}	0.42240x10 ⁻² 0.99440	0.41142x10 ⁻² 0.99440	0.41142x10 ⁻² 0.99440	0.41142x10 ⁻² 0.99440	0.41142x10 ⁻² 0.99440	0.41142x10 ⁻² 0.99440	0.41142x10 ⁻² 0.99440	0.41142x10 ⁻² 0.99440	0.41142x10 ⁻² 0.99440	0.41142x10 ⁻² 0.99440	0.41142x10 ⁻² 0.99440	0.41142x10 ⁻² 0.99440	0.41142x10 ⁻² 0.99440	0.41142x10 ⁻² 0.99440	0.41142x10 ⁻² 0.99440	0.41142x10 ⁻² 0.99440	0.99023 0.99916
10^{-12}	0.41142x10 ⁻² 0.99440	0.14847x10 ⁻² 0.99440	0.14847x10 ⁻² 0.99440	0.14847x10 ⁻² 0.99440	0.14847x10 ⁻² 0.99440	0.14847x10 ⁻² 0.99440	0.14847x10 ⁻² 0.99440	0.14847x10 ⁻² 0.99440	0.14847x10 ⁻² 0.99440	0.14847x10 ⁻² 0.99440	0.14847x10 ⁻² 0.99440	0.14847x10 ⁻² 0.99440	0.14847x10 ⁻² 0.99440	0.14847x10 ⁻² 0.99440	0.14847x10 ⁻² 0.99440	0.14847x10 ⁻² 0.99440	0.99024 0.99976
10^{-14}	0.14847x10 ⁻² 0.99440	0.32581 0.99440	0.32581 0.99437	0.32581 0.99437	0.32581 0.99437	0.32581 0.99437	0.32581 0.99437	0.32581 0.99437	0.32581 0.99437	0.32581 0.99437	0.32581 0.99437	0.32581 0.99437	0.32581 0.99437	0.32581 0.99437	0.32581 0.99437	0.32581 0.99437	0.99024 0.99998
10^{-16}	0.32581 0.99440	0.52903 0.99437	0.52903 0.99437	0.52903 0.99437	0.52903 0.99437	0.52903 0.99437	0.52903 0.99437	0.52903 0.99437	0.52903 0.99437	0.52903 0.99437	0.52903 0.99437	0.52903 0.99437	0.52903 0.99437	0.52903 0.99437	0.52903 0.99437	0.52903 0.99437	0.99024 0.99999

(2) Placement of observer poles: Based on the values of the measurement noise and plant noise covariances, i.e., $R_S = 10^{-6}I_0$, $Q_S = 10^{-10}I_0$, the minimum and maximum moduli of the A^* eigenvalues may be determined preliminarily from Table 4. In general, as for the design of the Kalman filter, the R and Q should satisfy the conditions: $R \geq R_S$, $Q \geq Q_S$. After these conditions have been satisfied, the location of the observer poles may be changed by means of the variation of parameters μ_R and μ_Q in Table 4. When $R = R_S$, $Q = Q_S$, the minimum and maximum moduli of the eigenvalues of A^* (observer) are 0.74399 and 0.99450, respectively.

(3) Placement of controller poles: As we know^[23] the minimum modulus of the observer closed-loop eigenvalues should be less than that of controller closed-loop eigenvalues, so that the estimator can provide accurate timely state information for the controller. Based on this principle, the possible appropriate modulus of the minimum controller eigenvalues for Case 7 (Table 3) is 0.86382, i.e., $R = 10^{-4}I_0$, the minimum and maximum modulus of the eigenvalues of A^* (controller) are 0.86382 and 0.98745 (Table 3).

(4) Certifying by simulation: In order to certify the preliminary design of the controller and observer, in addition to showing the LQG designed controlled response for this system, we also need to propose another kind of controller and observer placement for comparing with the above preliminary design.

2.5. Digital Simulation

The simulation of the LQG digital control of the orbiting shallow spherical shell system is considered here including some controllers and observers. The software package, ORACLS,^[24] has been used for implementation.

It is assumed that the measurement accuracy of the displacement sensors is about the order of 1 centimeter for the shell deflection, and the modelling error for the dynamical system is less than the error of the measurement sensors. The covariance matrices used for the simulation of both the sensor measurement and system (plant) noise are determined as follows:

$R_S = 10^{-6}I_0$ is the covariance of the measurement noise used in the simulation and $Q_S = 10^{-10}I_0$ is the covariance of the system (plant) noise used.

Now let $w(i)$ be the system noise used in the Kalman filter model, then

$$E\{w(i)\} = 0 \text{ and } E\{w(i)v^T(j)\} = Q\delta_{ij}$$

Define $v(i)$ as the observational noise used in the Kalman filter model. Similarly,

$$E\{v(i)\} = 0 \text{ and } E\{v(i)v^T(j)\} = R\delta_{ij}$$

Initial state simulation is then

$$x(0) = \bar{x}(0) + w_0 \quad \bar{x}(0) = E\{x(0)\}$$

$$P_0 = E\{w_0 w_0^T\}$$

The initial conditions are assumed as

$$\bar{x}_1(0) = \psi(0) = 0.0, \quad \bar{x}_2(0) = \phi(0) = 0.1, \quad \bar{x}_3(0) = \theta(0) = 0.1$$

$$\bar{x}_4(0) = \varepsilon_1(0) = 0.01, \quad \bar{x}_5(0) = \bar{x}_6(0) = \dots = \bar{x}_{18}(0) = 0.0$$

and the initial values of the estimated state are assumed to be zero, i.e.,

$$x_1(0/-1) = 0.0, \quad x_2(0/-1) = 0.0,$$

$$x_3(0/-1) = \dots = x_{18}(0/-1) = 0.0.$$

In order to study the influence of different numbers of actuators on the LQG control process and the influence of different locations for a given number of actuators on the LQG control process, Cases 2, 4, 6, 7 (Table 2) are selected for simulation. The minimum modulus of the eigenvalues of A^* for the four cases are 0.91717, 0.86701, 0.90319, 0.86383, respectively, but the minimum modulus of the eigenvalues of A^* are the same, i.e., 0.74399. The transient response under the LQG optimal digital control for Cases 2, 4, 6, 7 are shown in Figures 2-5. It is evident that the transient response of Case 7 is the best among Cases 2, 4, 6, 7, because there are more actuators for Case 7 and the degree of controllability for Case 7 is also the highest among the four cases. It is valuable to point out the fact that the transient response of Case 6 is worse than that of Case 4 even though the number of actuators in Case 6 is greater than those in Case 4. The reason is that eight actuators for Case 6 are all located on the same nodal circle ($\xi = \text{const.}$) and the influence of the control forces along the same nodal circle on the displacement at the other nodal circles are very weak. In view of the degree of controllability, it is also easily understandable. The degree of controllability of Case 6 is less than that of Case 4.

In summary, the locations of the actuators should be as far as possible from the nodal meridians, and also should be arranged so that as few actuators as possible will be located on the same nodal circle.

As we pointed out in Ref. [23], an appropriate design of LQG optimal control systems should require that the minimum modulus of the eigenvalue of the LQG closed-loop observer should be less than the minimum modulus of the eigenvalue of the LQG closed-loop controller, so that the estimator can provide accurate timely state information for the controller. In order to certify again this fact, four combinations of observer/controller pole locations (EC-1, EC-2, EC-3, EC-4)

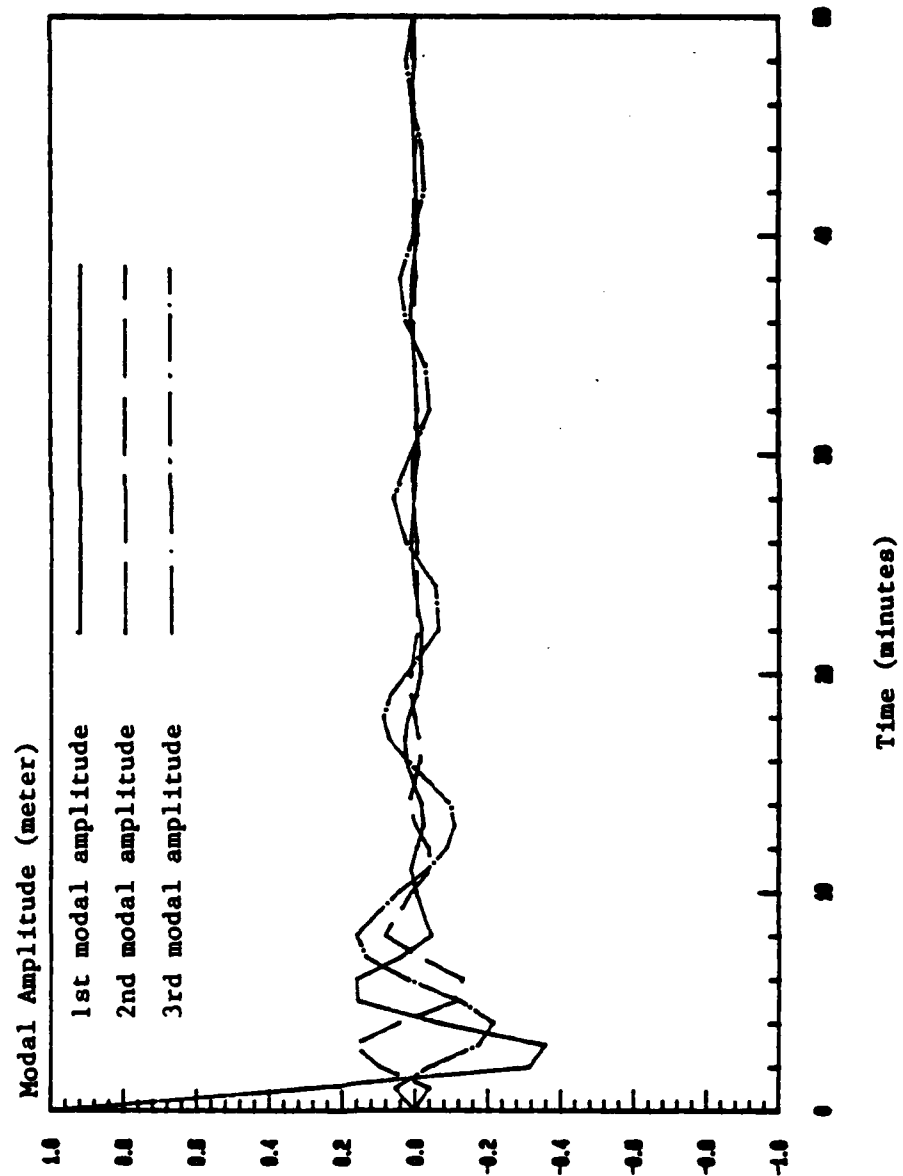


Figure 2. LQG Control of Shallow Spherical Shell Transient Response for Case 2

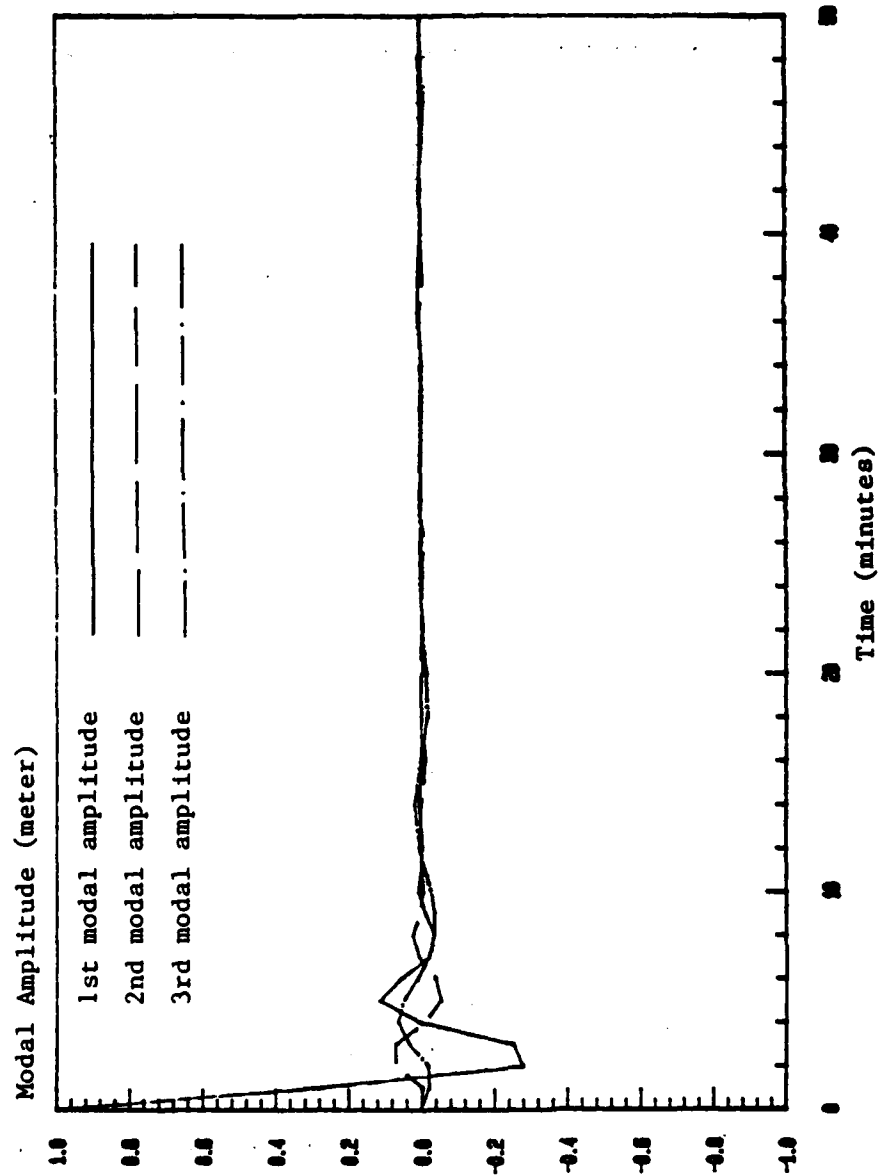


Figure 3. LQG Control of Shallow Spherical Shell Transient Response for Case 4

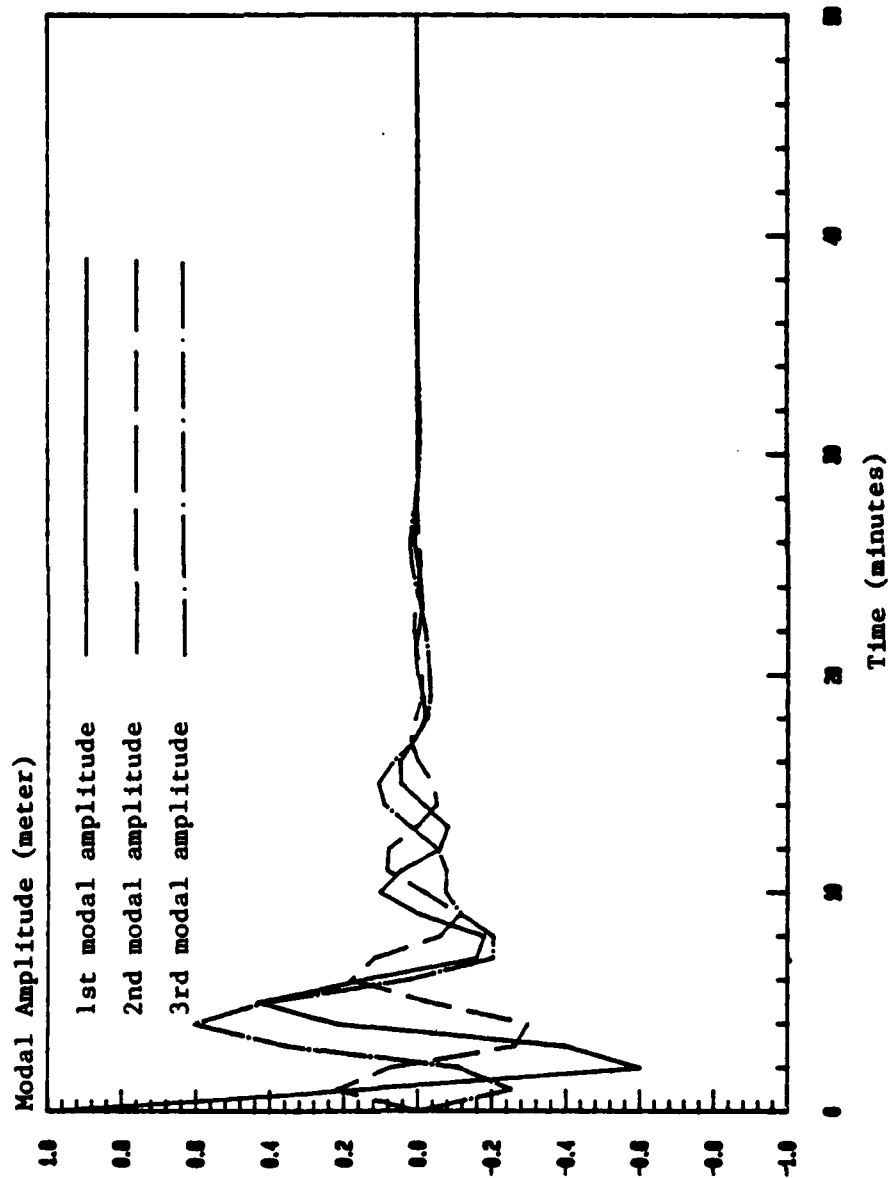


Figure 4. LQG Control of Shallow Spherical Shell Transient Response for Case 6

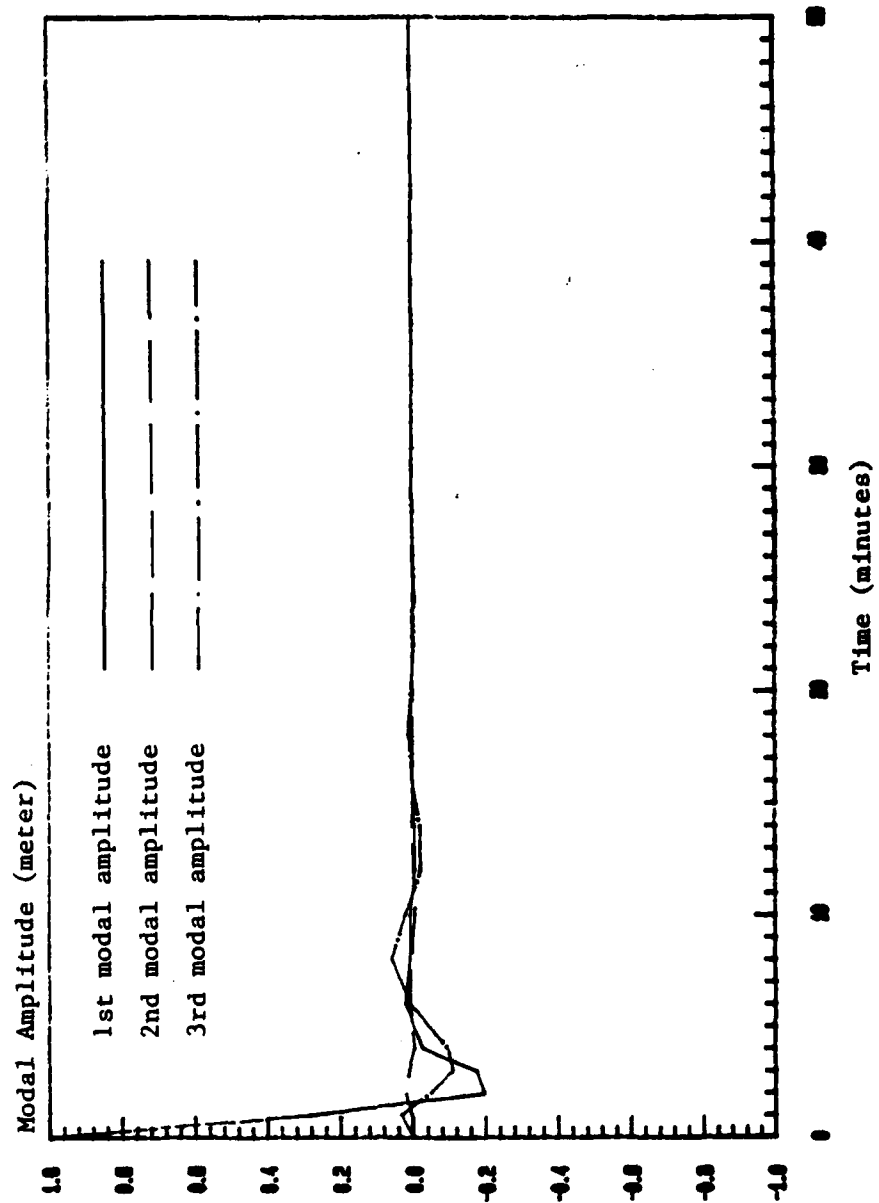


Figure 5. LQG Control of Shallow Spherical Shell Transient Response for Case 7

described in Table 5 are proposed for simulation based on Case 7 (12 actuators, see Table 2).

The transient responses of the LQG optimal digital control of the shallow spherical shell for EC-1 to EC-4 are shown in Figures 6-10. It is evident that the transient response of attitude and modal amplitude for EC-1 are the worst (Figures 6 and 7). These transient responses do not converge, because the minimum modulus of the observer eigenvalues is greater than the minimum modulus of the controller eigenvalue; thus the estimator cannot provide the timely accurate estimate of the state. The transient response of EC-2 is better, because the minimum modulus of the observer eigenvalues is less than that of the controller, so the observer can provide the accurate timely state estimate (Figure 8). It is expected that EC-3 and EC-4 both can provide appropriate timely state estimates for the controller, (Figures 9, 10) but the terminal part of the transient response of the estimate and control for EC-4 is degraded (note the lack of smoothness in Figure 10). The appearance of this phenomenon is due to the small ratio, μ_R/μ_Q , so that Kalman filter becomes too sensitive to the new observational data with the actual measurement noise. Therefore, the relationship between the locations of the controller and observer poles for EC-2 and EC-3 are better.

2.6. Conclusions

The analysis and design of the optimal LQG digital shape and orientation control for an orbiting shallow spherical shell system are presented. The emphasis in this paper is placed on the analysis and design of LQG optimal digital controllers and observers for the orbiting flexible shallow spherical shell system. As for the placement of the controller and observer poles the minimum modulus of the eigenvalue of the closed-loop observer must be less than the minimum modulus of the eigenvalues of the closed-loop controller, so that the observer can provide the accurate estimate of the state variables for the controller. When placing the positions of the controller and observer poles to meet the above requirement, we should also pay attention that the ratio μ_R/μ_Q cannot be too small; otherwise the Kalman filter becomes too sensitive to the new observational data so that state estimate will not be so smooth.

The problems of determining the number and location of the actuators are also studied by means of the concept of the degree of controllability together with transient response simulations. For the model of the orbiting shell treated here 12 actuators properly placed can provide both shape and orientation control. Actuators placed along the edge of the shell should be capable of providing thrust both tangentially and normal to the base of the shell.

TABLE 5. THE PARAMETERS OF THE SYSTEM EC1 - EC4

Combination of Obser./Contr.	$\hat{R} = \mu_C I_0$	$R = \mu_R I_0$	$Q = \mu_Q I_0$	Min. Modulus of Eigenvalues	Min. Modulus of Eigenvalues
Poles	μ_C	μ_R	μ_Q	of A^*	of \hat{A}^*
EC-1	10^{-4}	10^{-6}	10^{-16}	0.86383	0.99402
EC-2	10^{-4}	10^{-6}	10^{-10}	0.86383	0.74399
EC-3	10^{-4}	10^{-6}	10^{-6}	0.86383	0.32581
EC-4	10^{-4}	10^{-6}	10^{-4}	0.86383	0.14847×10^{-2}

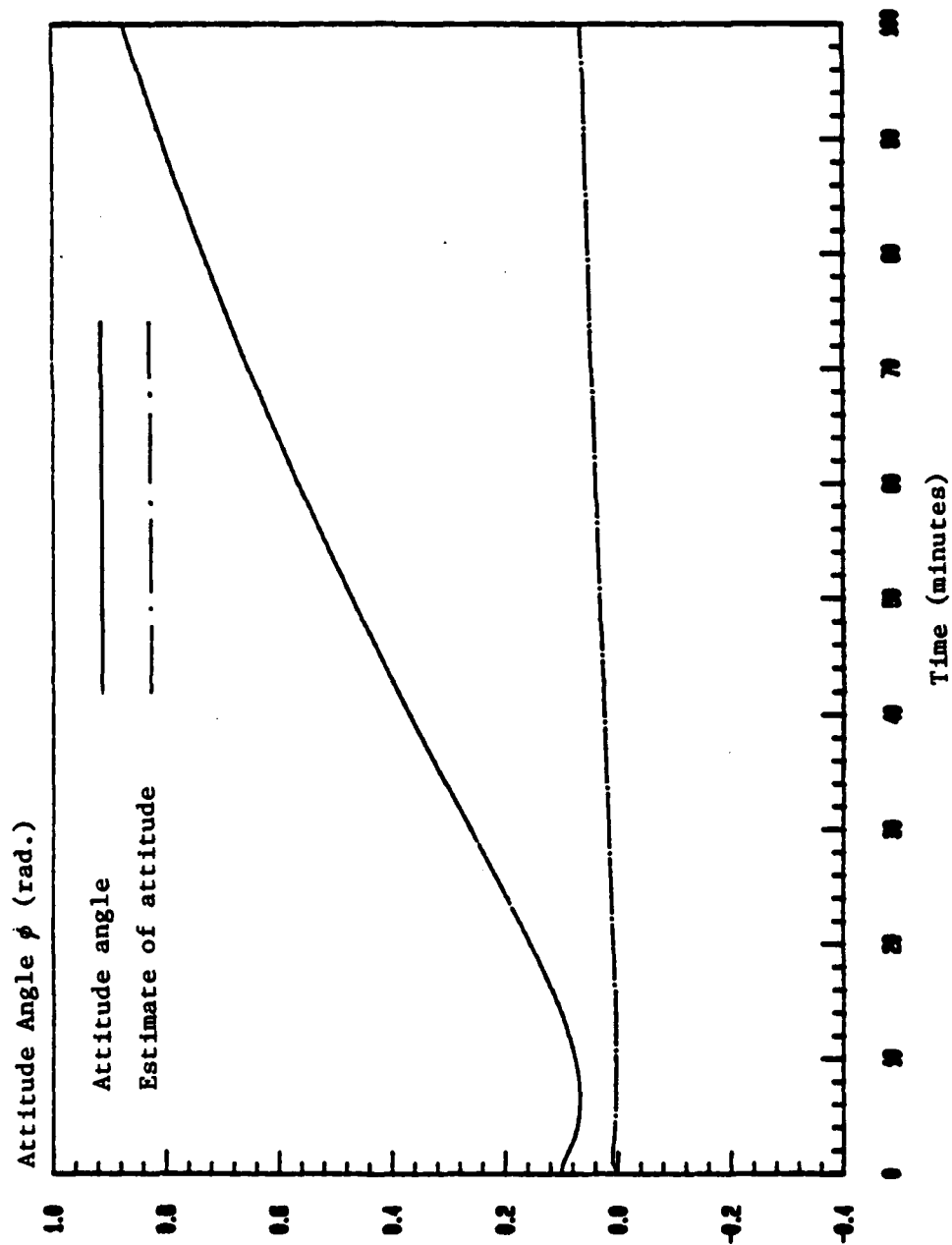


Figure 6. LQG Control of Shallow Spherical Shell Transient Response for System EC-1(a)

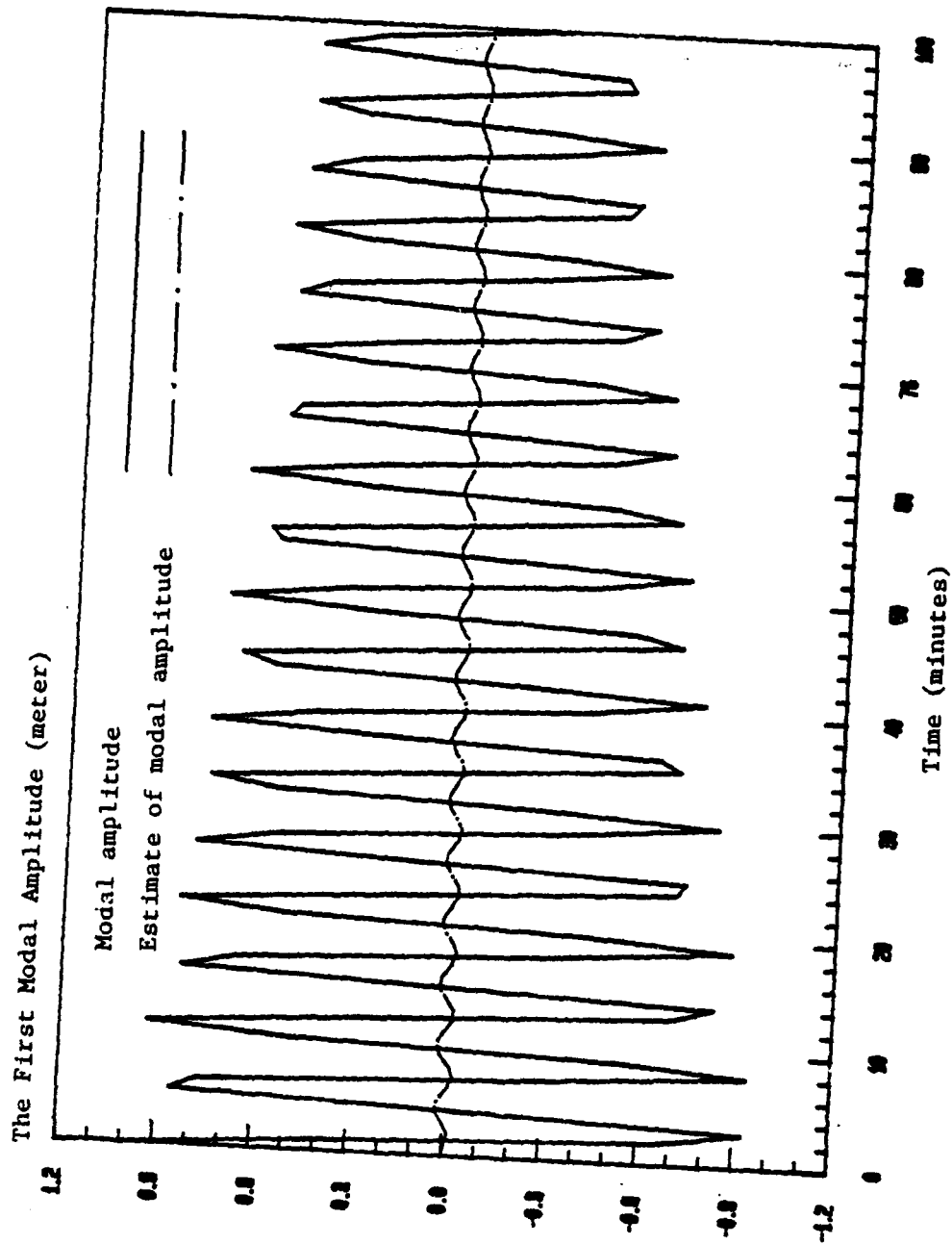


Figure 7. LQG Control of Shallow Spherical Shell Transient Response for System EC-1(b)

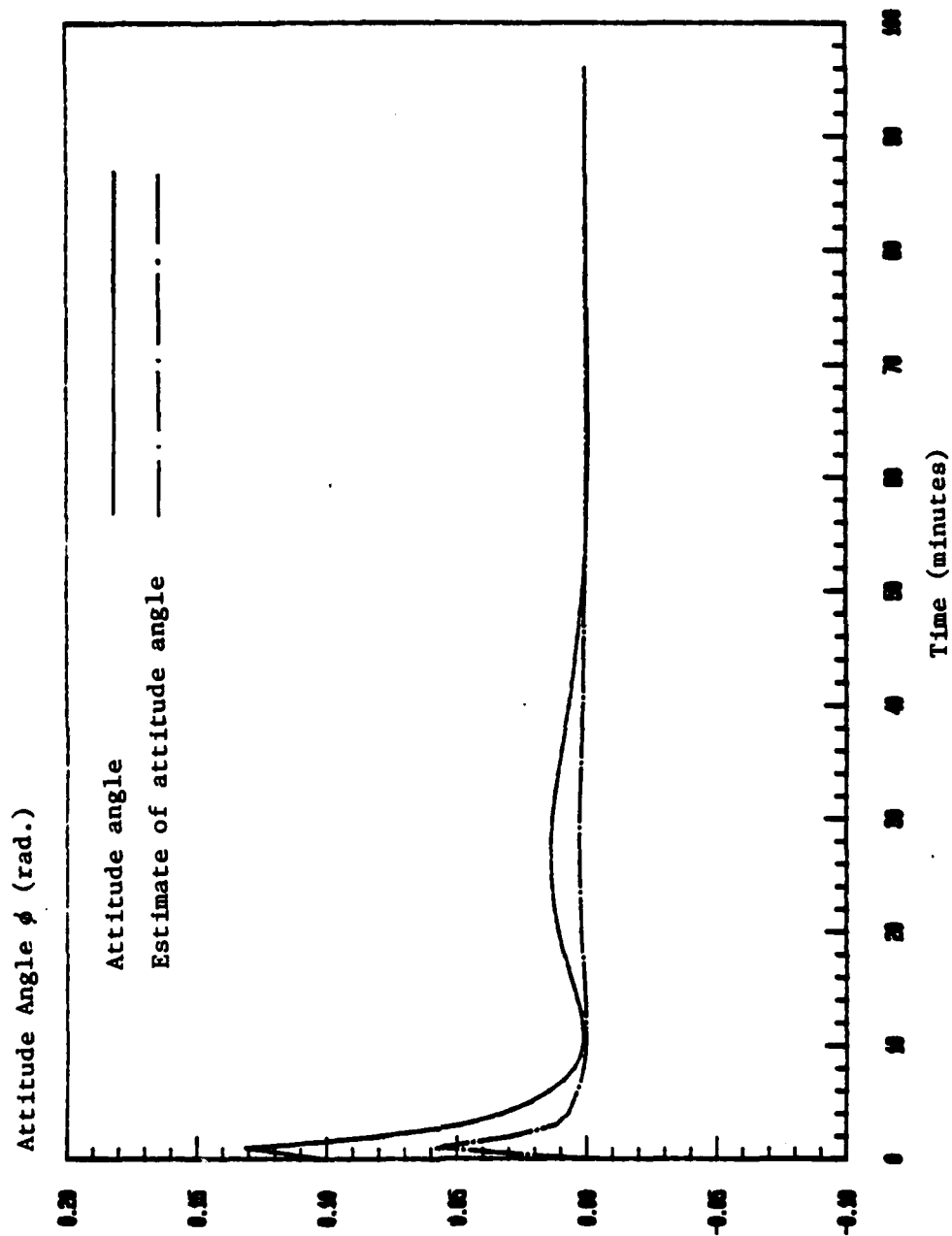


Figure 8. LQG Control of Shallow Spherical Shell Transient Response for System EC-2

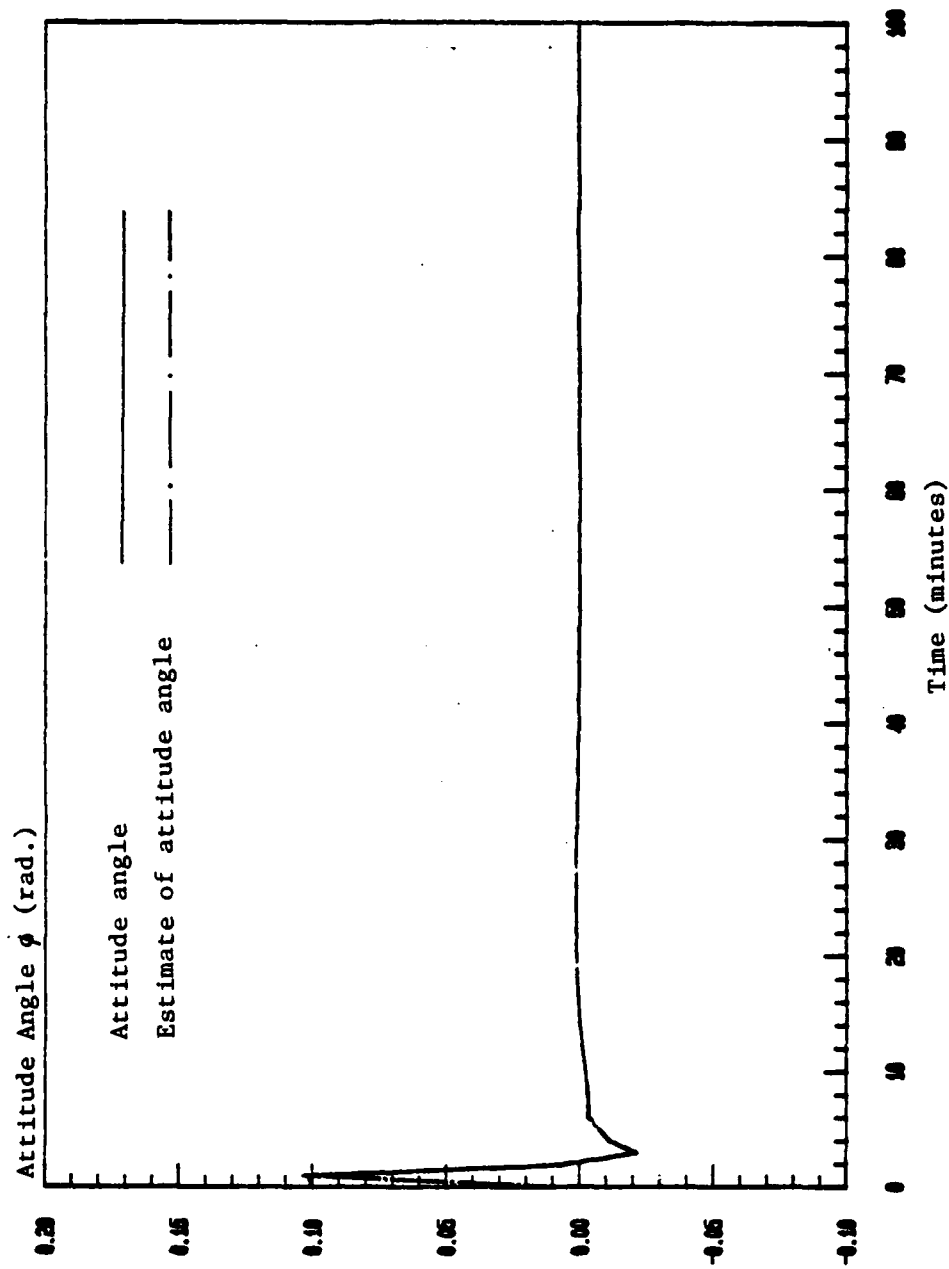


Figure 9. LQG Control of Shallow Spherical Shell Transient Response for System EC-3

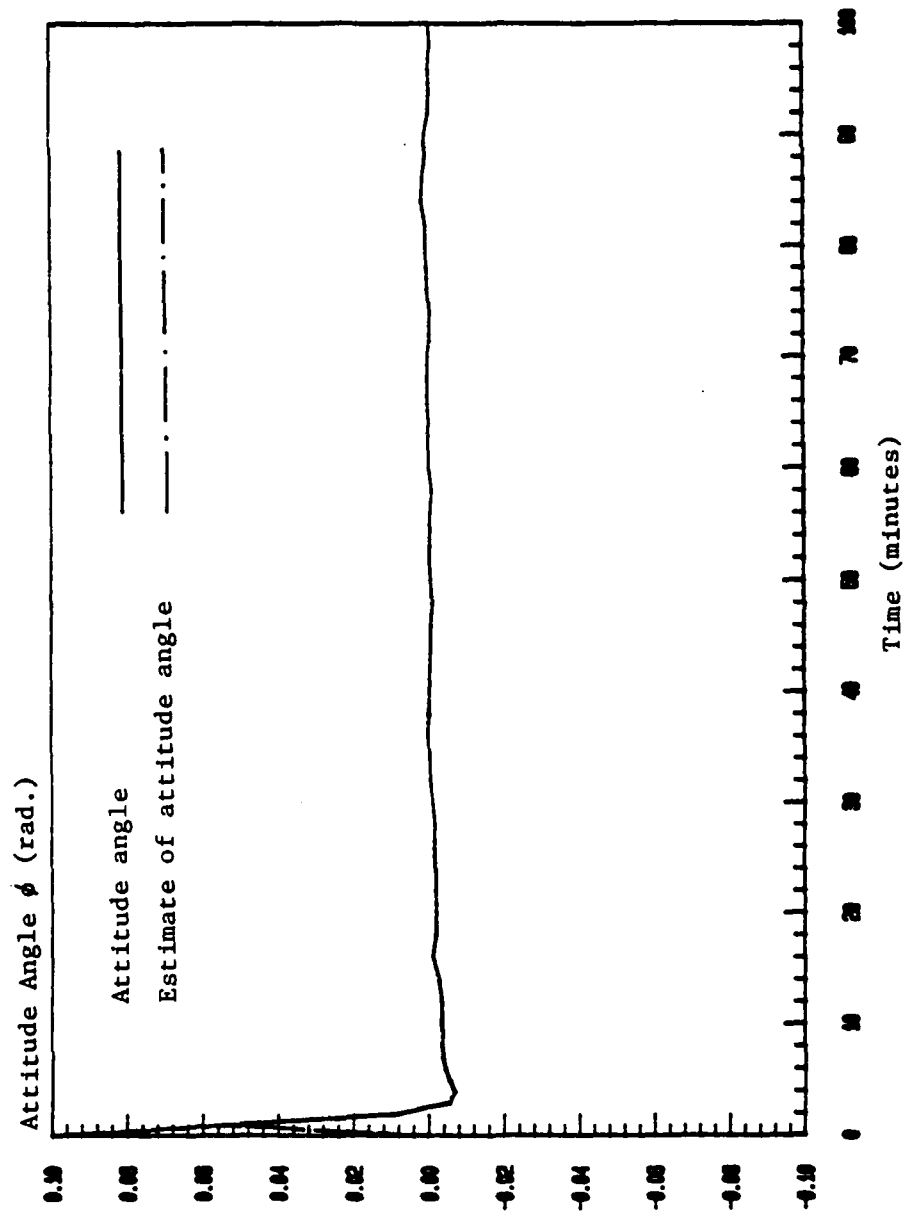


Figure 10. LQG Control of Shallow Spherical Shell Transient Response for System EC-4

3. SOME DEFINITIONS OF DEGREE OF CONTROLLABILITY (OBSERVABILITY) FOR DISCRETE-TIME SYSTEMS AND THEIR APPLICATIONS

3.1. Introduction

The concept of controllability is one of the cornerstones of modern control theory. Yet despite its fundamental importance from a theoretical point of view, its practical utility for control system either controllable or it is uncontrollable. There is no provision for consideration of the more subtle question: how controllable is the system?

The desirability of a degree of controllability (earlier it was called the controllability index) concept has been recognized in the literature since 1961 when Kalman, Ho and Narendra^[25] discussed it. Early papers in the area^[26-28] concentrated on particular properties of either the controllability Grammian matrix or the controllability matrix itself in developing definitions of the degree of controllability. It is natural to try to connect the degree of controllability to properties of the standard controllability matrix $P_c = (B:AB: \dots A^{n-1}B)$, and define the degree of controllability as the square root of the minimum eigenvalue of $P_c P_c^T$. In 1979 Viswanathan, Longman and Likins considered the "shortcomings" of this definition^[29]. Four apparent difficulties with this definition must somehow be handled before the definition becomes "viable"; therefore, they presented a new definition of the degree of controllability of a control system by means of a scalar measure based on the concept of the "recovery region."

In this paper three candidate definitions of degree of controllability, which were presented first by Muller and Weber^[28] for linear continuous systems, are presented for linear discrete-time systems based on the scalar measure of the Grammian matrix. The three candidates for the degree of observability of linear discrete-time systems are also presented. Because some difficulties with this definition (as pointed out by Viswanathan^[29] have been handled here, and the degree of controllability (observability) based on a scalar measure of the Grammian matrix can be readily calculated, the three candidates for the degree of controllability (observability) are viable for practical engineering design.

The emphasis of this paper is in showing the physical and geometrical meanings and the general properties of the three candidate definitions of degree of controllability (observability) as physically meaningful measures. The concepts of degree of controllability are applied to the actuator placement problem for the orbiting shallow spherical shell control system. The degree of controllability for seven cases in which the placement of actuators are all different are compared. The LQG transient responses for several typical systems with different degrees of controllability are also shown.

3.2. Concept and Physical Meaning of Controllability

In order to show the physical meaning of the degree of controllability, first of all, we consider the fuel optimal problem for the

linear discrete-time system. The state equations are as follows:

$$x(k_i) = \phi(k_i, k_{i-1})x(k_{i-1}) + \Gamma(k_{i-1})u(k_{i-1}) \quad (40)$$

$$(i = 1, 2, \dots, N)$$

The fuel optimal control problem can be stated as follows: To find the system control $u(k_{i-1})$ ($i = 1, 2, \dots, N$) which can transfer from the initial state $x(k_0)$ to the final state of the system $x(k_N) = 0$ during the time interval $[k_0, k_N]$, and such that the performance index,

$$J_N = \sum_{i=1}^N \langle u(k_{i-1}), u(k_{i-1}) \rangle \quad (41)$$

is minimized.

Equation (40) may be written

$$x(k_N) = \phi(k_N, k_0)x(k_0) + \sum_{i=1}^N \phi(k_N, k_i) \Gamma(k_{i-1}) u(k_{i-1}) \quad (42)$$

or

$$x(k_N) - \phi(k_N, k_0) x(k_0) = T_p U \quad (43)$$

where

$$T_p = (\Gamma(k_{N-1}) : \phi(k_N, k_{N-1})\Gamma(k_{N-2}) : \dots : \phi(k_N, k_0)\Gamma(k_0)) \quad (44)$$

$$U = \begin{pmatrix} u(k_{N-1}) \\ u(k_{N-2}) \\ \vdots \\ u(k_0) \end{pmatrix} \quad (45)$$

Considering the requirement that $x(k_N)=0$, Equation (43) may be written:

$$-x(k_0) = P_c U \quad (46)$$

where

$$P_c = \phi(k_0, k_N) T_p \quad (47)$$

and the fuel optimal problem becomes the following conditional extremum problem

$$\inf \{ \|U\|^2 \mid P_c U(\cdot) = -x(k_0) \} \quad (48)$$

where $\|\cdot\|$ represents the Euclidian norm. This problem can be solved by using the Lagrange multiplier method. If λ is the

Lagrange multiplier, the problem stated in Equation 48 is equivalent to the general problem of extremizing the following cost function

$$J_p = \langle U, U \rangle - \lambda^T (P_c U + x(k_0))$$

In order for J_p to be an extremum the following necessary conditions must be satisfied:

$$\begin{aligned} \frac{\partial J_p}{\partial U} &= 2U - P_c^T \lambda = 0 \\ \frac{\partial J_p}{\partial \lambda} &= P_c U + x(k_0) = 0 \end{aligned} \quad (49)$$

i.e.,

$$\begin{aligned} (P_c P_c^T) \lambda &= -2x(k_0) \\ 2U &= P_c^T \lambda \end{aligned} \quad (50)$$

If the system is controllable, then the inverse of the matrix, $(P_c P_c^T)$, exists, and the optimal control, U^* , is

$$U^* = -P_c^T (P_c P_c^T)^{-1} x(k_0) \quad (51)$$

After substituting Equation 51 into the performance index, Equation 41, the minimum control energy is obtained as follows:

$$\begin{aligned} J_N^* &= \langle U^*, U^* \rangle = \langle -P_c^T (P_c P_c^T)^{-1} x(k_0), -P_c^T (P_c P_c^T)^{-1} x(k_0) \rangle \\ &= \langle (P_c P_c^T)^{-1} x(k_0), x(k_0) \rangle \end{aligned} \quad (52)$$

$$J_N^* = x^T(k_0) W_c^{-1}(k_N, k_0) x(k_0) \quad (53)$$

where, $W_c(k_N, k_0) = P_c P_c^T$

From intuitive considerations, the linear system "1" is more controllable than the linear system "2" if the energy, J_{N1}^* , required by system "1" for transferring the initial state, $x(k_0)$, to the final state $x(k_N) = 0$, is less than the energy required by the second system, J_{N2}^* , for transfer between the same initial and final states within the same time period, or stated mathematically,

$$x^T(k_0) W_{c1}^{-1}(k_N, k_0) x(k_0) \leq x^T(k_0) W_{c2}^{-1}(k_N, k_0) x(k_0) \quad \forall x(k_0) \in \mathbb{R}^n \quad (54)$$

Because $W_{c1}^{-1}(k_N, k_0)$ and $W_{c2}^{-1}(k_N, k_0)$ are two symmetrical positive definite matrices, the relationship (54) should be satisfied for any initial condition, $x(k_0) \in \mathbb{R}^n$; this implies that

$$W_{c1}^{-1}(k_N, k_0) \leq W_{c2}^{-1}(k_N, k_0) \quad (55)$$

or

$$W_{c1}(k_N, k_0) \geq W_{c2}(k_N, k_0) \quad (56)$$

Considering the symmetry of the matrices, W_{c1} and W_{c2} , the following relationships should be satisfied:

$$\lambda_1(W_{c1}^{-1}) \leq \lambda_1(W_{c2}^{-1}) \quad (i = 1, \dots, n) \quad (57)$$

or

$$\lambda_1(W_{c1}) \geq \lambda_1(W_{c2}) \quad (i = 1, \dots, n) \quad (58)$$

where $\lambda_1(W_{c1}^{-1})$, $\lambda_1(W_{c2}^{-1})$, $\lambda_1(W_{c1})$, $\lambda_1(W_{c2})$ are the i th eigenvalues of the matrices, W_{c1}^{-1} , W_{c2}^{-1} , W_{c1} and W_{c2} , respectively. It is evident from Equation 53 that the loci of equicontrol effort ($J^* = \text{constant}$) is a superellipsoid and its equation ($J_N^* = 1$) in the principal axis system is as follows:

$$\frac{x_1^2}{\frac{1}{\lambda_1(W_{c1}^{-1})}} + \frac{x_2^2}{\frac{1}{\lambda_2(W_{c1}^{-1})}} + \dots + \frac{x_n^2}{\frac{1}{\lambda_n(W_{c1}^{-1})}} = 1 \quad (59)$$

Considering the relationship between $\lambda_1(W_{c1}^{-1})$ and $\lambda_1(W_c)$:

$$\lambda_1(W_{c1}^{-1}) = \frac{1}{\lambda_{n+1-i}(W_c)} \quad (60)$$

i.e.,

$$\lambda_1(W_{c1}^{-1}) < \lambda_2(W_{c1}^{-1}) < \dots < \lambda_n(W_{c1}^{-1})$$

$$\begin{aligned} \lambda_1(W_c) &= \frac{1}{\lambda_n(W_{c1}^{-1})} < \lambda_2(W_c) = \frac{1}{\lambda_{n-1}(W_{c1}^{-1})} \\ &< \dots < \lambda_n(W_c) = \frac{1}{\lambda_1(W_{c1}^{-1})} \end{aligned}$$

Then Equation 59 can be written as follows:

$$\frac{x_1^2}{\lambda_1(W_c)} + \frac{x_2^2}{\lambda_2(W_c)} + \dots + \frac{x_n^2}{\lambda_n(W_c)} = 1 \quad (61)$$

Therefore, from the geometrical viewpoint, it is clear from Equations 54 and 61 that if system "1" is more controllable than system "2," each axis of the superellipsoid for system "1" is longer than the corresponding axis for the system "2." The square root of each of the eigenvalues of the matrix, W_c , is just the length of the corresponding superellipsoid principal axis.

3.3 Three Candidates for the Definitions of Degree of Controllability and Their General Properties

As we see in Equation 54, in terms of the matrices this comparison of the costs of two systems leads to (56), i.e.,

$$W_{c1}(k_N, k_0) \geq W_{c2}(k_N, k_0) \quad (56)$$

which means that $W_{c1} - W_{c2}$ has to be a positive semidefinite matrix. The matrix condition (56) is equivalent to "n" scalar conditions and, therefore, a simple scalar quantity cannot be employed to describe the conditions (56). For engineering purposes it is desirable to replace the matrix measure by a scalar figure of merit [25]. There are three obvious candidates for such scalar measures:

the maximum eigenvalue of $W_c^{-1}(k_N, k_0)$, the trace of $W_c^{-1}(k_N, k_0)$, and the determinant of $W_c(k_N, k_0)$ [28]. The significance of these quantities is shown in the following section:

(1) The first candidate for the degree of controllability, μ_1 . As shown in (54), we must consider the values of the control effort $x^T(k_0)W_c^{-1}(k_N, k_0)x(k_0)$ $\forall x(k_0) \in R^n$ when comparing the control effort of the two systems. It is natural to use the maximum control effort,

$$\begin{aligned} \text{Max} \quad & x^T(k_0)W_c^{-1}(k_N, k_0)x(k_0) \\ ||x(k_0)|| &= 1 \\ x(k_0) &\in R^n \end{aligned} \quad (62)$$

as a scalar measure of the control effort. It is well known that the scalar quantity defined in (62) is just the maximum eigenvalue, $\lambda_{\max}(W_c^{-1})$, of the matrix W_c^{-1} , and the $\lambda_{\max}(W_c^{-1})$ is just the reciprocal of the minimum eigenvalue of the matrix, W_c , i.e.,

$$\text{Max } x^T(k_0)W_c^{-1}(k_N, k_0)x(k_0) = \lambda_{\max}(W_c^{-1}) = \frac{1}{\lambda_{\min}(W_c)} \quad (63)$$

$$\begin{aligned} ||x(k_0)|| &= 1 \\ x(k_0) &\in R^n \end{aligned}$$

where the $\lambda_{\min}(W_c)$ is the minimum eigenvalue of the matrix, $W_c(k_N, k_0)$. For the reasons given above, we may define the degree of controllability, μ_1 , as follows:

$$\mu_1 = \lambda_{\min}(W_c(k_N, k_0)) = \sigma_{\min}^2(P_c) \quad (64)$$

This definition means that as μ_1 increases, then the control effort decreases. It is evident that the square root of the degree of controllability defined by Equation (64) is just the minimum semiaxis of the superellipsoid defined by Equation (61) (it can be called the degree of controllability superellipsoid). If $\mu_1 = 0$, the system will not be controllable.

(2) The second candidate for the degree of controllability, μ_2 . Similar to (62), we can also use the average value of the control effort, $x^T(k_0)W_c^{-1}x(k_0)$, over the unit hypersphere $\{x(k_0): ||x(k_0)|| = 1\}$

$$\frac{\int_{\|x(k_0)\| = 1} x^T(k_0) W_c^{-1} x(k_0) dx(k_0)}{\int_{\|x(k_0)\| = 1} dx(k_0)}$$

as a scalar measure of the control effort. After integrating, it can be obtained [28]

$$\frac{\int_{\|x(k_0)\| = 1} x^T(k_0) W_c^{-1} x(k_0) dx(k_0)}{\int_{\|x(k_0)\| = 1} dx(k_0)} = \frac{1}{n} \text{tr} W_c^{-1} \quad (65)$$

where n is the order of the state. Therefore, we may define the second candidate for the degree of controllability as follows:

$$\mu_2 = \frac{n}{\text{tr} W_c^{-1}(k_N, k_0)} \quad (66)$$

For practical applications it is desirable to maintain the average cost Equation (65) as small as possible. Hence, the measure, μ_2 , has to be as large as possible. The definition (66) of a measure instead of (65) is more convenient because uncontrollable systems are characterized by a vanishing value of μ_2 , which arises from a limiting process.

(3) The third candidate of degree of controllability, μ_3 . The third possible candidate for a scalar quantitative measure of controllability is the determinant of $W_c(k_N, k_0)$ because the volume of controllability superellipsoid $x^T(k_0) W_c^{-1}(k_N, k_0) x(k_0) = 1$ is proportional to the square root of the determinant of $W_c(k_N, k_0)$:

$$\text{Vol} = \int_{x(k_0)^T W_c^{-1} x(k_0) \leq 1} dx(k_0) = \text{Const.} \sqrt{\det W_c} \quad (67)$$

Therefore, we may define the third candidate definition of degree of controllability as follows:

$$\mu_3 = (\det W_c(k_N, k_0))^{1/n} \quad (68)$$

From geometrical considerations, $2^n (\mu_3)^{n/2}$ is just the volume of the hyperrectangular parallelepiped whose sides are the axes of the hyperellipsoid. The larger, μ_3 , the more controllable the system is; the uncontrollable system is also characterized by $\mu_3 = 0$.

(4) The general properties of the degree of controllability. In the previous sections we gave the definitions of degree of controllability and their physical and geometry meaning. The degrees of controllability, as a scalar measure, are invariant under an orthogonal similarity transformation. The proof will be given in the Appendix of this paper. In addition, they are scalar quantities defined over the cone set, W_c^* , of positive definite and semidefinite matrices.

Their properties are as follows [28]:

- (a) $\mu_1(W_c) = 0$ ($i = 1, 2, 3$) for $W_c \in W_c^*$ with $\det W_c = 0$, i.e., the system cannot be controllable;
- (b) $\mu_1(W_c) > 0$ ($i = 1, 2, \dots, N$) for $W_c \in W_c^*$ with $\det W_c > 0$;
- (c) $\mu_1(\lambda W_c) = \lambda \mu_1(W_c)$ ($i = 1, 2, 3$) for $\lambda \geq 0$, $W_c \in W_c^*$;
- (d) $\mu_1(W_c) \geq \mu_1(W_{c1}) + \mu_1(W_{c2})$ ($i = 1, 2, 3$) for $W_c = W_{c1} + W_{c2}$, $W_{c1}, W_{c2} \in W_c^*$.

The proof of the properties (a) - (d) will be given in the Appendix of this paper.

The physical meaning of the properties (a) - (c) are evident. The physical meaning of property (d) is that the degree of controllability for the system which contains two control elements is higher than the sum of the degrees of controllability for the two systems each of which contain only a single controller.

The μ_1 , μ_2 , μ_3 are three kinds of candidates for the degree of controllability, the physical meanings of which are different. The following relationship among μ_1 , μ_2 and μ_3 can be stated [28]:

$$\mu_1 \leq \mu_2 \leq \mu_3 \quad (69)$$

The sufficient and necessary condition for the equality to be true is that all of the eigenvalues of W_c be equal.

3.4. The Definition of Degree of Observability and Its Physical Meaning

Suppose the dynamical equations and observational equations are as follows:

$$x(k_1) = \Phi(k_1, k_{1-1})x(k_{1-1}) + \Gamma(k_{1-1})u(k_{1-1}) \quad (70)$$

$$y(k_{1-1}) = H(k_{1-1})x(k_{1-1}) + v(k_{1-1}) \quad (i = 1, 2, \dots, N) \quad (71)$$

where $v(k_{1-1})$ is observational white noise with statistical properties

$$E v(k_{1-1}) = 0 \quad E \{v(k_{1-1})v^T(k_{1-1})\} = R_{1-1} \quad (i = 1, 2, \dots, N).$$

Equation (70) may be written in another form in terms of the initial state as follows:

$$x(k_1) = \Phi(k_1, k_0)x(k_0) + \sum_{j=1}^1 \Phi(k_1, k_j)\Gamma(k_{j-1})u(k_{j-1}) \quad (72)$$

$$y(k_{1-1}) = H(k_{1-1})\Phi(k_{1-1}, k_0)x(k_0)$$

$$+ H(k_{i-1}) \sum_{j=1}^{i-1} \Phi(k_{i-1}, k_j) \Gamma(k_{j-1}) u(k_{j-1}) + v(k_{i-1}) \quad (73)$$

(i = 1, 2, \dots, N)

When i assumes values from 1 through N, Equation (73) can be put in a matrix form as follows:

$$Y = P_0 x(k_0) + V \quad (74)$$

where

$$Y = \begin{bmatrix} y(k_0) \\ y(k_1) - H(k_1) \Gamma(k_0) u(k_0) \\ \vdots \\ y(k_{N-1}) - H(k_{N-1}) \sum_{j=1}^{N-1} \Phi(k_{N-1}, k_j) \Gamma(k_{j-1}) u(k_{j-1}) \end{bmatrix}$$

$$P_0 = \begin{bmatrix} H(k_0) \\ H(k_1) \Phi(k_1, k_0) \\ \vdots \\ H(k_{N-1}) \Phi(k_{N-1}, k_0) \end{bmatrix}$$

$$V = \begin{bmatrix} v(k_0) \\ v(k_1) \\ \vdots \\ v(k_{N-1}) \end{bmatrix}$$

$$E\{V\} = 0 \quad E\{VV^T\} = \begin{bmatrix} R_0 & & & \\ & R_1 & & \\ & & \ddots & \\ & & & R_{N-1} \end{bmatrix} = R$$

We consider the weighted least square estimate problem, the performance index of the weighted least square estimate is

$$J = (Y - P_0 x(k_0))^T R^{-1} (Y - P_0 x(k_0)) \quad (75)$$

It is well known that the weighted least square estimate $\hat{x}(k_0)$ is

$$x(k_0) = (P_0^T R^{-1} P_0)^{-1} P_0^T R^{-1} Y \quad (76)$$

The estimate error is

$$\begin{aligned} x(k_0) - \hat{x}(k_0) &= (P_0^T R^{-1} P_0)^{-1} P_0^T R^{-1} (P_0 x(k_0) - Y) \\ &= -(P_0^T R^{-1} P_0)^{-1} P_0^T R^{-1} V \end{aligned}$$

The covariance of the estimate error is

$$E\{(x(k_0) - \hat{x}(k_0))(x(k_0) - \hat{x}(k_0))^T\} = (P_0^T R^{-1} P_0)^{-1} \quad (77)$$

When $R = I$, the covariance of the least square estimate error is just

$$E\{(x(k_0) - \hat{x}(k_0))(x(k_0) - \hat{x}(k_0))^T\} = (P_0^T P_0)^{-1} = W_0^{-1} \quad (78)$$

where

$$W_0 = P_0^T P_0 \quad (79)$$

Similar to the degree of controllability, we call the W_0 the degree of the observability matrix. The three kinds of definitions of degree of observability are as follows:

$$\mu_1(W_0) = \lambda_{\min}(W_0) \quad (80)$$

$$\mu_2(W_0) = \frac{n}{\text{tr} W_0^{-1}} \quad (81)$$

$$\mu_3(W_0) = (\det W_0)^{1/n} \quad (82)$$

Because the W_0^{-1} is the covariance matrix of the least square estimate, then the $\text{tr} W_0^{-1}$ is the sum of the squares of the variances associated with the least square error estimate, so the physical meaning of $\mu_2(W_0)$ is evident. $\mu_1(W_0)$ is the maximum eigenvalue of the covariance error matrix W_0^{-1} for the least square estimate. $\mu_3(W_0)$ is the reciprocal of the geometrical average of the error covariance matrix eigenvalues for the least square estimate.

In general, if the estimation accuracy of system "1" is higher than that of system "2," it means

$$W_{01}^{-1} \leq W_{02}^{-1} \quad (83)$$

It implies

$$W_{01} \geq W_{02}, \quad \text{tr} W_{01}^{-1} \leq \text{tr} W_{02}^{-1} \quad (84)$$

and

$$\lambda_i(W_{01}) > \lambda_i(W_{02}) \quad (i = 1, 2, \dots, n) \quad (85)$$

Therefore

$$\mu_1(W_{01}) \geq \mu_1(W_{02})$$

$$\mu_2(W_{01}) \geq \mu_2(W_{02})$$

$$\mu_3(W_{01}) \geq \mu_3(W_{02})$$

i.e., the degrees of observability defined by (80-82) for system "1" are all higher than the corresponding degrees of observability for system "2."

3.5. The Degree of Controllability (Observability) for Discrete-Time Invariant Systems

Let the dynamical system and observational system for the discrete time-invariant system be described as follows:

$$x(k_1) = \Phi x(k_1 - 1) + \Gamma u(k_1 - 1) \quad (86)$$

$$y(k_1) = Hx(k_1) + v(k_1) \quad (87)$$

The degree of controllability matrix W_c for the system (86), (87) is

$$W_c = P_c P_c^T \quad (88)$$

where

$$P_c = (\Gamma: \Phi\Gamma: \dots: \Phi^{n-1}\Gamma) \quad (89)$$

The degree of observability matrix for system (86), (87) is

$$W_0 = P_0^T P_0 \quad (90)$$

where

$$P_0 = \begin{pmatrix} H \\ H\Phi \\ \vdots \\ H\Phi^{n-1} \end{pmatrix} \quad (91)$$

The three kinds of definitions of degree of controllability are as follows:

$$\mu_1(W_c) = \lambda_{\min}(W_c) \quad (92)$$

$$\mu_2(W_c) = \frac{n}{\text{tr} W_c^{-1}} \quad (93)$$

$$\mu_3(W_c) = (\det W_c)^{1/n} \quad (94)$$

Similarly, the three kinds of degree of observability are as follows:

$$\mu_1(W_0) = \lambda_{\min}(W_0) \quad (95)$$

$$\mu_2(W_0) = \frac{n}{\text{tr} W_0^{-1}} \quad (96)$$

$$\mu_3(W_0) = (\det W_0)^{1/n} \quad (97)$$

3.6. Application

We would like to use the concepts of the degree of controllability for the actuator placement problem of the shallow spherical shell. The motion equations for a shallow spherical shell in orbit subject to external forces and torques are as follows [19]:

$$\dot{X} = AX + Bu \quad (98)$$

where

$$A = \begin{pmatrix} 0 & I \\ -\bar{A} & D \end{pmatrix} \quad B = \begin{pmatrix} 0 \\ \bar{B} \end{pmatrix}$$

$$X = (\psi, \phi, \theta, \epsilon_1, \epsilon_2, \dots, \epsilon_6, \dot{\psi}, \dot{\phi}, \dot{\theta}, \dot{\epsilon}_1, \dot{\epsilon}_2, \dots, \dot{\epsilon}_6)^T$$

$$u = (|f_1|, |f_2|, \dots, |f_\alpha|)^T$$

$$\varepsilon_i = q_i(t)/l \quad (i = 1, 2, \dots, 6)$$

$$B = \begin{pmatrix} \frac{-l_{z1}f_{y1} + l_{y1}f_{z1}}{J_x(0)\omega_c^2}, \frac{-l_{z2}f_{y2} + l_{y2}f_{z2}}{J_x(0)\omega_c^2}, \dots, \frac{-l_{z\alpha}f_{y\alpha} + l_{y\alpha}f_{z\alpha}}{J_x(0)\omega_c^2} \\ \frac{-l_{y1}f_{x1} + l_{x1}f_{y1}}{J_z(0)\omega_c^2}, \frac{-l_{y2}f_{x2} + l_{x2}f_{y2}}{J_z(0)\omega_c^2}, \dots, \frac{-l_{y\alpha}f_{x\alpha} + l_{x\alpha}f_{y\alpha}}{J_z(0)\omega_c^2} \\ \frac{l_{z1}f_{x1} - l_{x1}f_{z1}}{J_y(0)\omega_c^2}, \frac{l_{z2}f_{x2} - l_{x2}f_{z2}}{J_y(0)\omega_c^2}, \dots, \frac{l_{z\alpha}f_{x\alpha} - l_{x\alpha}f_{z\alpha}}{J_y(0)\omega_c^2} \\ \frac{\phi_x^{(1)}(\xi_1, \beta_1)}{M_1 l \omega_c^2}, \frac{\phi_x^{(1)}(\xi_2, \beta_2)}{M_1 l \omega_c^2}, \dots, \frac{\phi_x^{(1)}(\xi_\alpha, \beta_\alpha)}{M_1 l \omega_x^2} \\ \vdots \\ \frac{\phi_x^{(6)}(\xi_1, \beta_1)}{M_6 l \omega_c^2}, \frac{\phi_x^{(6)}(\xi_2, \beta_2)}{M_6 l \omega_c^2}, \dots, \frac{\phi_x^{(6)}(\xi_\alpha, \beta_\alpha)}{M_6 l \omega_x^2} \end{pmatrix}$$

ψ, ϕ, θ yaw, roll and pitch angles, respectively, of the undeformed axis of the shallow spherical shell.

$q_i(t)$ modal amplitude of the i th generic mode whose shape function is $\phi_x^{(i)}$

ω_c orbital angular rate, constant for assumed circular orbit

l characteristic length (the base radius)

M_i i th modal mass

$\phi_x^{(i)}$ the x -axis component of the i th modal shape function

l_{xi}, l_{yi}, l_{zi} the components of the moment arm for the i th actuator

Equation 98 is nondimensionalized according to

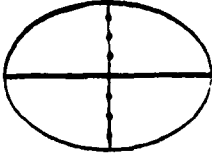
$$\tau = \omega_c t, \varepsilon_i = q_i(t)/l \quad (i = 1, 2, \dots, 6)$$

The derivative in Equation 98 is with respect to τ .

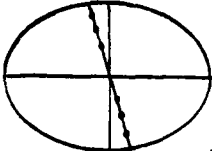
If we use six actuators to control the orientation and shape of the shallow spherical shell, the arrangement of the six actuators may be assumed for the following seven cases (Table 6):

TABLE 6. THE ACTUATOR LOCATIONS (ξ , θ) AND FORCE DIRECTIONS (f_x , f_y , f_z)

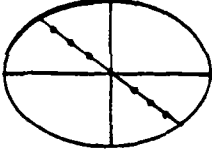
CASE 1

Actuator No.	ξ	θ	f_x	f_y	f_z	Location of Actuator
1	0.28	0°	1	0	0	
2	0.57	0°	1	1	0	
3	0.84	0°	1	1	1	
4	0.28	180°	1	0	0	
5	0.57	180°	1	1	0	
6	0.84	180°	1	1	1	

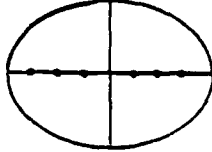
CASE 2

Actuator No.	ξ	θ	f_x	f_y	f_z	Location of Actuator
1	0.28	5°	1	0	0	
2	0.57	5°	1	1	0	
3	0.84	5°	1	1	1	
4	0.28	185°	1	0	0	
5	0.57	185°	1	1	0	
6	0.84	185°	1	1	1	

CASE 3

Actuator No.	ξ	θ	f_x	f_y	f_z	Location of Actuator
1	0.28	45°	1	0	0	
2	0.57	45°	1	1	0	
3	0.84	45°	1	1	1	
4	0.28	225°	1	0	0	
5	0.57	225°	1	1	0	
6	0.84	225°	1	1	1	

CASE 4

Actuator No.	ξ	θ	f_x	f_y	f_z	Location of Actuator
1	0.28	90°	1	0	0	
2	0.57	90°	1	1	0	
3	0.84	90°	1	1	1	
4	0.28	270°	1	0	0	
5	0.57	270°	1	1	0	
6	0.84	270°	1	1	1	

CASE 5

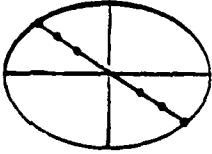
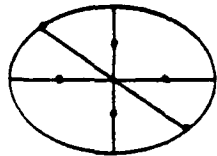
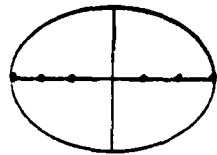
Actuator No.	ξ	θ	f_x	f_y	f_z	Location of Actuator
1	0.28	45°	1	0	0	
2	0.57	45°	1	0	0	
3	1.00	45°	1	$-\sin 45^\circ$	$\cos 45^\circ$	
4	0.28	225°	1	0	0	
5	0.57	225°	1	0	0	
6	1.00	225°	1	$\sin 45^\circ$	$-\cos 45^\circ$	

Table 6 (continued)

CASE 6

Actuator No.	ξ	β	f_x	f_y	f_z	Location of Actuator
1	0.57	0°	1	0	0	
2	0.57	90°	1	0	0	
3	0.57	180°	1	0	0	
4	0.57	270°	1	0	0	
5	1.00	45°	1	$-\sin 45^\circ$	$\cos 45^\circ$	
6	1.00	225°	1	$\sin 45^\circ$	$-\cos 45^\circ$	

CASE 7

Actuator No.	ξ	β	f_x	f_y	f_z	Location of Actuator
1	0.28	90°	1	0	0	
2	0.57	90°	1	0	0	
3	1.00	90°	1	-1	0	
4	0.28	270°	1	0	0	
5	0.57	270°	1	0	0	
6	1.00	270°	1	1	0	

The seven cases may be divided into two groups. The first group includes case 1 through case 4. The second group includes case 5 through case 7. In the first group there are six jets (actuators) for each case. In the second group there are six jets for each case, but two of the jets for the second group are located at the edge of the shell with their thrust direction tangent to the shell's (circular) edge. In order to reduce the possibility that the jets used primarily for shape control would also disturb the orientation of the shell, the placement of these jets are arranged symmetrically with respect to the shell's undeformed principal axes.

The values of the degree of controllability for each case are listed in Table 7. The reason why the degree of controllability for case 1 is zero is that all the actuators are located along the meridional nodal line of one of the fundamental shell vibrational modes.

In the first group of actuators, the best placement of actuators for which the degree of controllability is highest is case 4. In the second group, the best placement of actuators is case 7, and the degree of controllability for case 7 is also higher than that for case 4. The reason why the degree of controllability for case 6 is so low is that four actuators are all located on the same nodal circle ($\xi = \text{constant}$).

In summary, the locations of the actuators should be as far as possible from the nodal lines, and also should be arranged so that as few actuators as possible will be located on the same nodal circle.

In order to control the orientation of the shell effectively, a combination of tangential jets along the edge of the shell together with selected jets normal to the shell's major surface is recommended.

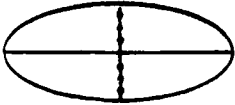
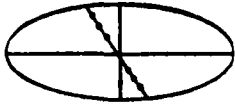
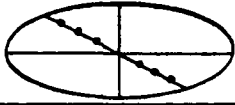
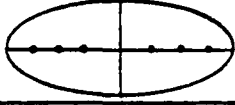


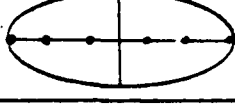
If the number of actuators is limited to six, the arrangement of actuators as in case 7 is suggested.

The transient responses with the LQG control for case 2 and case 7 are selected to show the differences in the attitude and the first three modal amplitude responses.

The initial conditions are the same for the two cases, i.e., roll $\phi(0) = 0.1$ rad., yaw $\psi(0) = 0.0$, pitch $\theta(0) = 0.1$ rad., the initial conditions for the first six modal amplitudes are $q_1(0) = 1$ meter, $q_2(t) = q_3(0) \dots = q_6(0) = 0.0$, respectively.

The transient response of the attitude motion for case 2 is shown in Figure 11, the transient responses of the 1st - 3rd modal amplitudes for case 2 are shown in Figure 12. The transient responses for the attitude motion and the modal amplitudes for case 7 are shown in Figure 13 and Figure 14, respectively. The comparison of the first modal amplitude responses for case 2 and case 7 is shown in Figure 15.

TABLE 7. THE DEGREE OF CONTROLLABILITY FOR THE DIFFERENT CASES

Case	Location of Actuator	μ_1	μ_2	μ_3
1		0.0	0.0	0.0
2		0.13875×10^{-12}	0.17646×10^{-11}	0.67227×10^{-7}
3		0.17673×10^{-11}	0.23696×10^{-10}	0.25045×10^{-6}
4		0.17974×10^{-11}	0.26434×10^{-10}	0.31558×10^{-6}
5		0.14332×10^{-10}	0.12421×10^{-9}	0.70448×10^{-6}
6		0.48360×10^{-12}	0.46915×10^{-11}	0.61384×10^{-6}
7		0.14332×10^{-10}	0.14788×10^{-9}	0.10084×10^{-5}

It is shown in Figures 11-15 that the roll is coupled strongly with yaw, but the coupling of roll, yaw with pitch is very weak. The quality of the transient responses of case 2 is much worse than that of case 7. This is a result of the differences in the degree of controllability for case 2 and case 7.

3.7. Conclusions

Three candidate definitions of the degree of controllability and observability are presented for linear discrete-time systems based on the scalar measure of the Grammian matrix. Their general properties, together with the physical and geometrical interpretations for the fuel optimal control problem are shown in detail. The advantages of these kinds of definitions for the degree of controllability (observability) are the clarity of the physical and geometrical interpretations and the simplicity of the resulting calculation. Thus, they are very useful for practical engineering design.

The transient responses for several typical systems with different degrees of controllability show that the quality of the system transient response depends on its degree of controllability: transient responses of the system with a higher degree of controllability are better than those of the system with a lower degree of controllability. The applications of the concept of the degree of controllability for actuator placement of the orbiting shallow spherical shell system are successfully implemented in this paper.

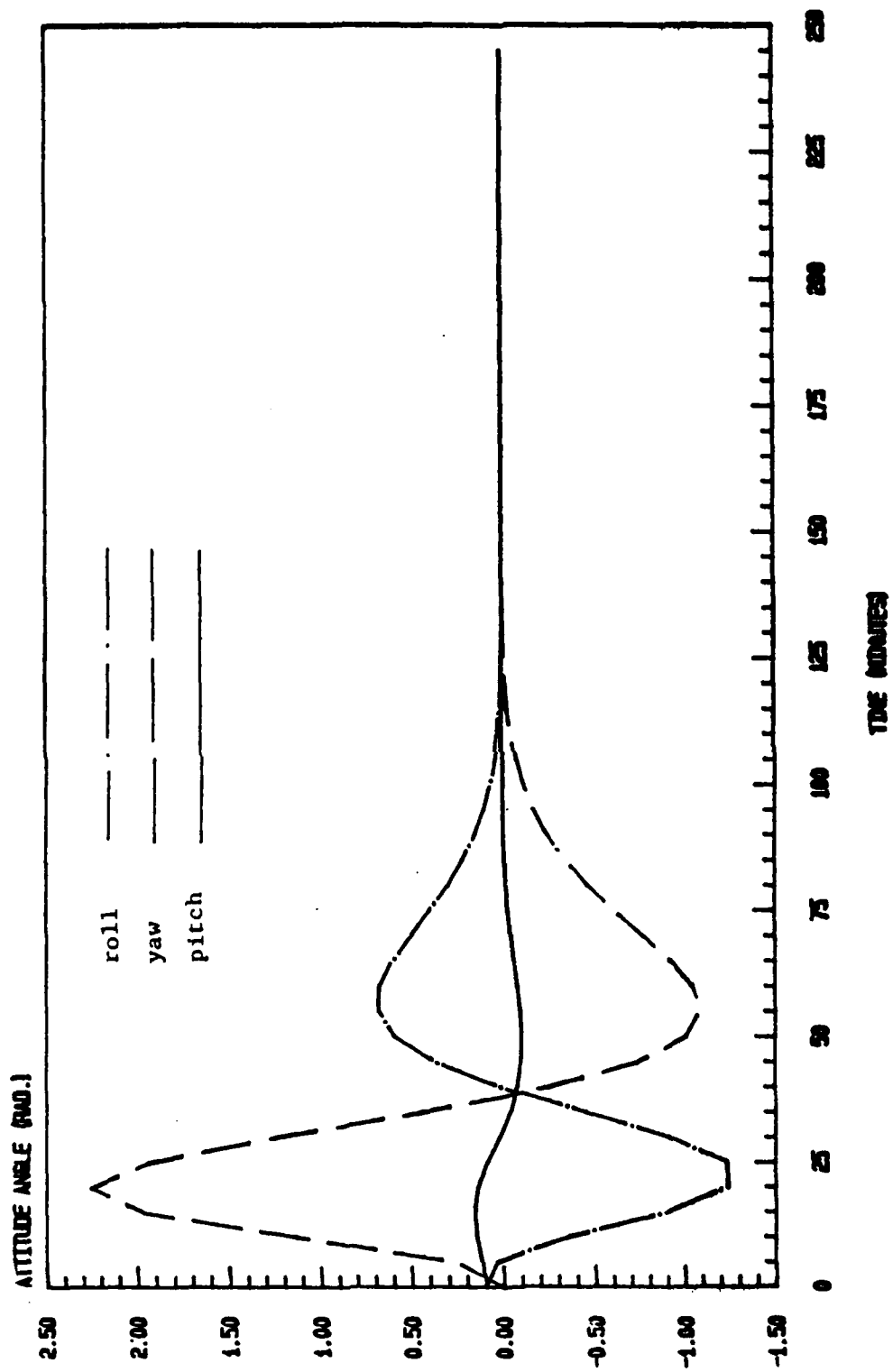


Figure 11. LQG Control of Shallow Spherical Shell Transient Response for Case 2 a (six actuators)

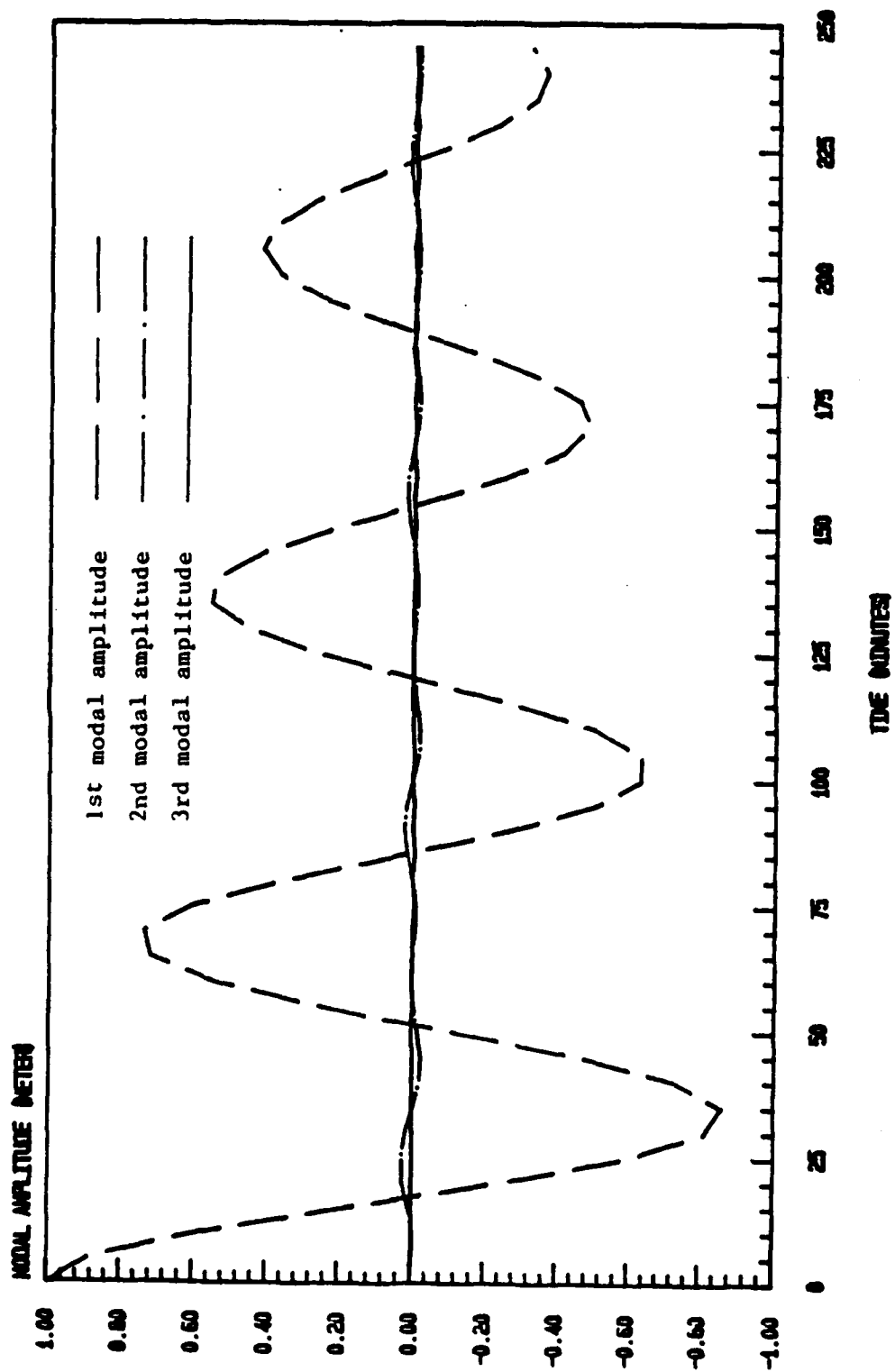


Figure 12. LQG Control of Shallow Spherical Shell Transient Response for Case 2 - b (six actuators)

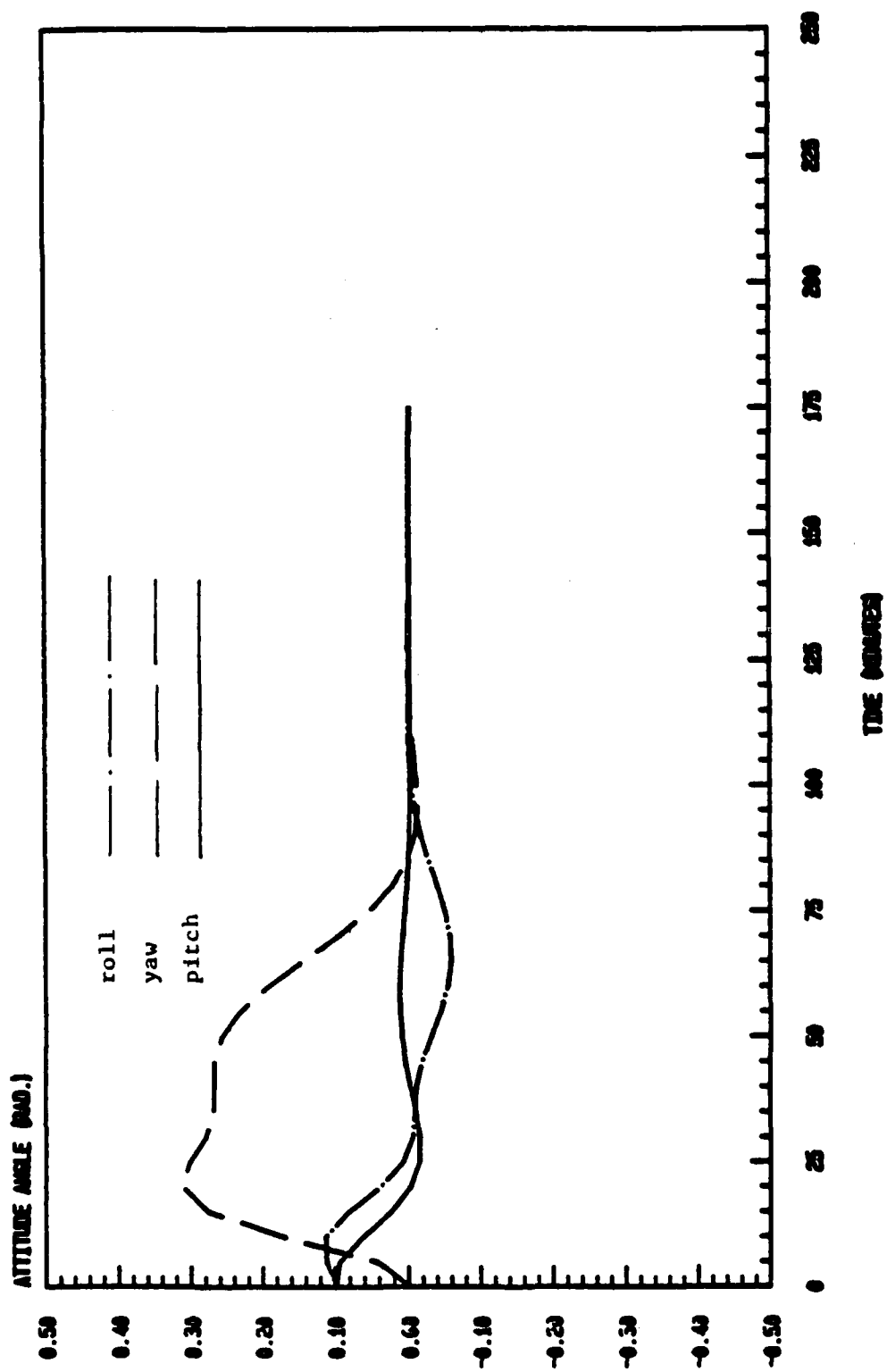


Figure 13. LQG Control of Shallow Spherical Shell Transient Response for Case 7 - a (six actuators)

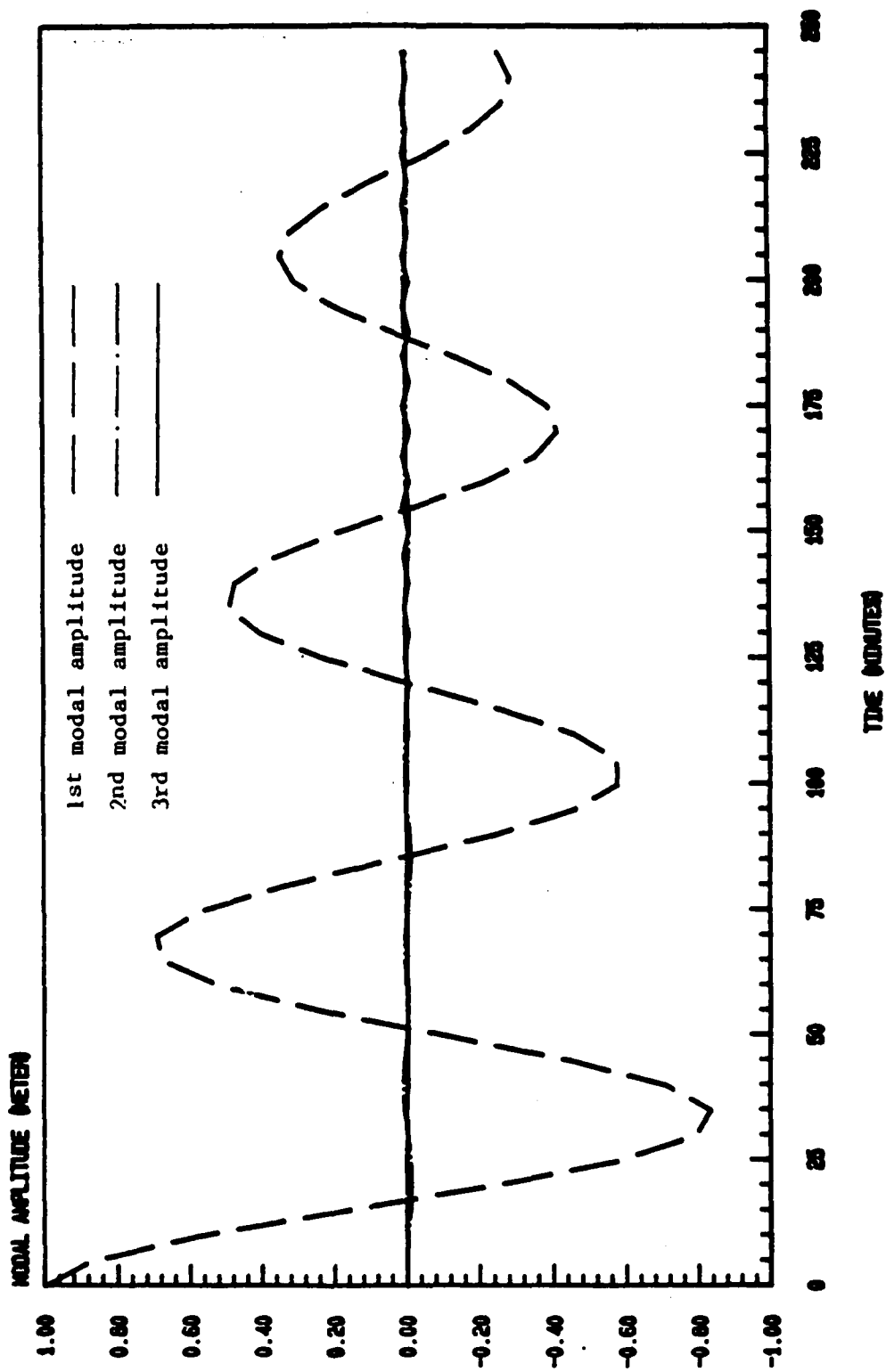


Figure 14. LQG Control of Shallow Spherical Shell Transient Response for Case 7 - b (six actuators)

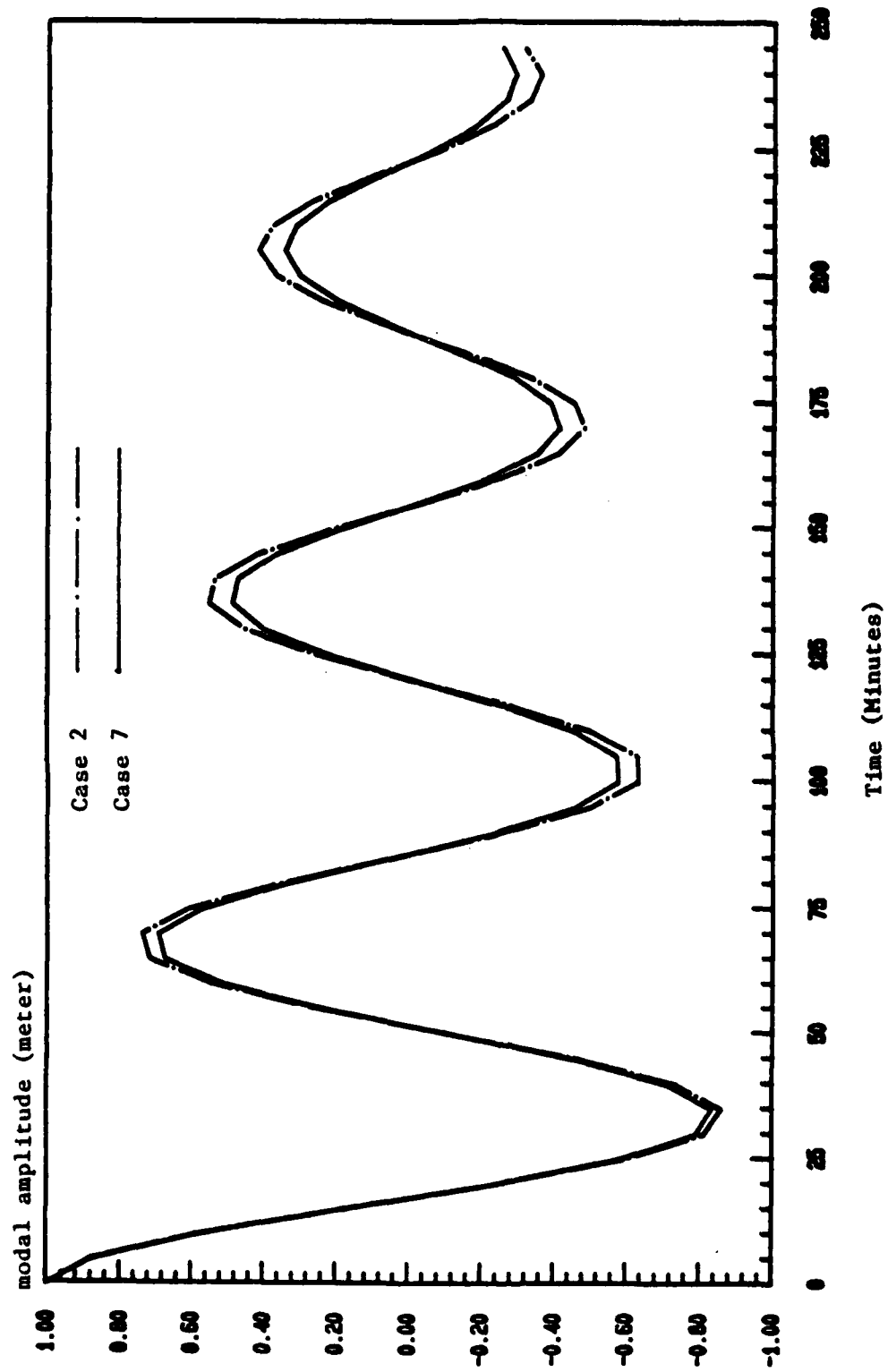


Figure 15. The First Modal Amplitude for Case 2 and Case 7

4. OPTIMAL DIGITAL CONTROL FOR FREE-FREE ORBITING PLATFORMS

4.1. Specific Aims

To develop practical design methods using LQR digital controllers and estimators for a third flexible orbiting plate, focusing on the analysis of the closed loop dynamics of the platform subject to discrete time input data.

4.2. Justification

Large flexible spacecraft systems have been proposed for future applications in widespread communication, electronic orbital based mail systems, and as collector of solar energy for transmittal to Earth-based receiving stations. For such missions, with the inherent size and necessary low weight to area ratio, the flexible parts of such systems must be treated as nonrigid. To satisfy the requirements of these proposed missions, both orientation and shape of the orbiting system should be controllable.

Often the optimal control laws for this system are developed under the assumption that the state vector is observed directly or the state information can be estimated on a continuous basis. However, for future applications the observational data will often be collected on a sampled basis, creating a discrete-time data system. Then the amount of information collected may be reduced and the format of data input may be acquired more conveniently. For the case to be treated here only a deterministic system will be addressed, i.e., no random noise will be considered.

Therefore, it appears useful and timely to study the control problem of large orbiting space structural systems with discrete-time observational data. It is well known that the development of modern control theory and technology provides a strong tool for solving this kind of engineering problem. [30, 31] The LQR regulator technique [30, 31] is that strong tool for synthesizing linear system control laws. It can provide acceptable control performance once the state and penalty matrices are properly selected. It does not restrict the number of actuators to be equal to the number of degrees of freedom in the system. Although, the LQR method has been developed and widely applied, it is still not an easy task to apply it to the engineering design for the control of large space structural systems, especially for systems with sampled data input. There are still many specific problems to be investigated. These are the aims of this proposed research.

4.3 Methodology

By using a modified version of the general formulation of the dynamics of a general flexible orbiting body formulated by Santini, [32] the equations of motion for a free-free beam in orbit were developed. In order to gain insight into the dynamics of such a large flexible system, the equations of motion for a free-free beam in orbit were studied. [1] The motion of the generic point in the body was described as the combination of the rigid body motion plus a superposition of the elastic modes.

Assuming the center of mass follows a circular orbit and the pitch and the flexural deformations occur only within the orbital plane, it is seen that the pitch motion does not influence the elastic motion. Also, the pitch and the elastic modes are decoupled for large values of the square of the ratio of the structural modal frequency to the orbital angular rate. For small values of this ratio the elastic motion is governed by Hill's 3-term equation which can be approximated by a Mathieu equation. Using a Mathieu stability chart, the resulting stability was considered. For small amplitude flexural motion, the rigid body and elastic modes are modelled to the first order, thus linearizing the equations of motion. Subsequently, an extension was made to the forementioned formulation and was applied to a thin, flexible orbiting plate.[33]

The ability to accurately determine the frequencies and mode shapes is essential for the analysis and control of large orbiting structures. For an aluminum square plate four different frequency and mode shape approximation methods were analyzed:[2]

- 1) The approximate frequencies and mode shapes of a rectangular plate were derived from a formulation by Warburton.[34, 35]
- 2) The analytical results for a square plate were calculated from a method developed by Lemke.[36]
- 3) The frequencies and mode shapes were computed using a finite element program, STRUDL, written at M.I.T.[37]
- 4) The frequencies and mode shapes were computed using GT-STRUDL, an updated version of STRUDL written at Georgia Tech.[38]

It was found that GT-STRUDL obtained better results than STRUDL and produced accurate results for specific finite element input grid point locations (node), whereas the Warburton and Lemke methods could only afford approximate answers.

The attitude and shape control can now be achieved by placing point thrust actuators perpendicular to the main surface and the edge of the plate. The placement of the actuators on the main surface help control the shape deformation and the torque about two axes. The placement of the actuators along the edge of the plate help control the torque about the third axis. Their effects on the rigid body and elastic modes are modeled to the first order.[39] For this investigation, it will be assumed that the sensors and actuators are completely colocated with the actuators and that the system is completely observable.

Now the control laws for this system may be applied to obtain the optimal control feedback gains based on an application of the linear regulator problem for a discrete-time data system.[30, 31] The implementation of the LQR procedure will be accomplished by using the ORCLS routines.[24]

The theorem about choosing the length of the sampling period in order to guarantee controllability will be applied to select the sampling period.^[23] When the controllability of the continuous system is guaranteed, in order to maintain controllability for the discretized system the eigenvalues of the system must satisfy certain conditions. As for the signal reconstruction, the sampling period, ΔT should be as small as possible, but if the sampling time is too small, the computational requirements may exceed the computer speed.

Under normal operation, the onboard computer estimation and control must be finished processing all the input data during one sampling period, ΔT , i.e., the prediction of the state variable which will be used for the controller must be estimated in time before the beginning of the next sampling sequence. Therefore, the sampling period should be more than the minimum computational time required by the onboard microcomputer for the simulation of each step in the estimation and control process. The choice of sampling time is also constrained by the performance of its transient response, i.e., overshoot characteristics, settling time, steady state RMS errors, etc.

4.4 Expected Results

A comparative parametric study will be performed for a different sampling period, ΔT ; the final determination of the sampling period will depend on the compromise between several factors including the controllability, restoration of the discrete-time input signal, the limitation of hardware functions, and the quality of the transient responses.

Software such as that currently available in the ORACLS LQR package can be used to synthesize the control laws and simulate the transient responses and required control efforts.

4.5 Why

As we all know there have been several proposals for large space structures, such as the Space Station, large antennas, solar panel arrays, propulsion devices, etc. Often these modern spacecraft systems can be modeled as a square or rectangular plate — the base — with the attached appendages. The acquired knowledge from this proposed study will have a wide range of applicability in the area of three dimensional dynamics and control of large flexible space structures.

5. CONCLUDING COMMENTS

The analysis and design of optimal LQG digital shape and orientation control for an orbiting shallow spherical shell system has been studied. In designing for the placement of the controller and observer poles, it is seen that the minimum modulus of the eigenvalues of the closed-loop observer system must be less than the minimum modulus of the eigenvalues of the closed-loop controller, so that the observer can provide for a timely accurate estimate of the state variables for the controller.

The problem of determining the number and location of the actuators is also studied by means of three concept definitions for the degree of controllability. These definitions are based on the scalar measure of the controllability Grammian matrix for discrete-time systems, and are interpreted both physically and geometrically. LQG transient responses for several combinations of actuator placements verify the concept of degree of controllability in selecting the number and locations of the actuators.

This work is also being extended to the analysis and design of optimal LQR digital shape and orientation control of flexible orbiting platform systems.

It is suggested that future related research should concentrate on the development of practical design methods for ensuring the robust control of sampled data large flexible space systems. The main objective should be to guarantee a certain minimum level of performance and stability robustness in the presence of variations from the ideal design conditions, and under the influence of unmodelled (or incompletely modelled) disturbances. Specific applications to the dynamics and control of the orbiting shallow spherical shell and platform system could be emphasized.

6. REFERENCES

1. Bainum, Peter M. and Kumar, V.K., "The Dynamics and Control of Large Flexible Space Structures," Part B. Development of Continuous Model and Computer Simulation, Final Report, NASA Grant NSG-1414, CR No. 156976, Howard University, May 1978.
2. Bainum, Peter M. and Reddy, A.S.S.R., "The Dynamics and Control of Large Flexible Space Structures - Part A. Shape and Orientation Control Using Point Actuators," NASA Grant NSG-1414, Howard University, July 1979.
3. Bainum, Peter M., Reddy, A.S.S.R. and Krishna, R., "On the Controllability and Control Law Design for an Orbiting Large Flexible Antenna System," The 34th International Astronautical Congress, IAF 83-340.
4. Larson, V. and Litkins, P.W., "Optimal Estimation and Control of Elastic Spacecraft," Advances in Control and Dynamics Systems, Vol. 13, ed. E.T. Leondes, Academic Press, New York, 1977.
5. Balas, M.M., "Feedback Control of Flexible Systems," IEEE Transactions on Automatic Control, Vol. AC-23, No. 4, 1978, pp. 673-679.
6. Seltzer, S.M., "Dynamics and Control of Large Space Structures: An Overview," Journal of the Astronautical Sciences, Vol. 27, No. 2, April - June 1979, pp. 95-101.
7. Kuo, B.C., "Design of Digital Control Systems with State Feedback and Dynamic Output Feedback," The Journal of the Astronautical Sciences, Vol. 27, No. 2, April - June 1979, pp. 207-214.
8. Kosut, R.L., "Stability of LQR Modal Control of Large Space Structures," AIAA Guidance and Control Conference, August 19-21, 1981, Proc. Paper No. 81-1835, pp. 359-364.
9. Skelton, R.E., "On the Selection of Optimal Bandwidths for LSS Controller," 22nd ACC, 1982.
10. Williams, J.P. and Montgomery, R.C., "Simulation and Testing of Digital Control on a Flexible Beam," AIAA Guidance and Control Conference, San Diego, California, August 9-11, 1982, Proc. Paper No. 82-1569, pp. 403-409.
11. Kwakernaak, H. and Sivan, R., Linear Optimal Control Systems, John Wiley and Sons, Inc., New York, 1972.
12. Maybeck, P.S., Stochastic Models, Estimation and Control, Volume 3, Academic Press, New York, 1982.
13. Juang, J-N. and Rodriguez, G., "Formulation and Application of Large Structures Actuator and Sensor Placements," Proceedings of the Second VPI&SU/AIAA Symposium on Dynamics and Control of

Large Flexible Spacecraft, edited by L. Meirovitch, 1979, pp. 247-262.

14. Laskin, R.A., Longman, R.W. and Likins, P.W., "A Definition of the Degree of Controllability for Fuel-Optimal Systems," Proceedings of the Third VPI&SU/AIAA Symposium on Dynamics and Control of Large Flexible Spacecraft, edited by L. Meirovitch, 1981, pp. 1-14.
15. Xing, Guangqian, "Observable Degree and Accuracy of Various Attitude Determination for Spinning Satellite," IFAC/ESA Joint Symposium on Automatic Control in Space, July 5-9, 1982, The Netherlands, Preprint, pp. 177-185.
16. Dorato, P., "Theoretical Developments in Discrete-Time Control," Automatica, Vol. 19, No. 4, 1983, pp. 395-400.
17. Bainum, P.M., "Dynamics and Robust Control of a Sampled Data System for Large Space Structures," unsolicited proposal submitted by Howard University to Air Force Wright Aeronautical Laboratory (Flight Dynamics Lab.), May 1989.
18. Bainum, Peter, Kumar, V.K., Krishna, R. and Reddy, A.S.S.R., "The Dynamics and Control of Large Flexible Space Structures - IV," Final Report NASA Grant: NSG-1414, Suppl. 3, CR No. 165815, Howard University, August 1981.
19. Xing, Guangqian and Bainum, Peter M., "The Equations of Motion for a General Orbiting Large Space Flexible System," The Sixteenth International Symposium on Space Technology and Science, May 22-27, 1988, Sapporo, Hokkaido, Japan.
20. Xing, Guangqian and Bainum, Peter M., "Some Definitions of Degree of Controllability (Observability) for Discrete-Time Systems and their Applications," The 12th Biennial ASME Conference on Mechanical Vibrations and Noise, September 17-20, 1989, Montreal, Canada (invited paper).
21. Johnson, M.W. and Reissner, E., "On Transverse Vibrations of Shallow Spherical Shell," Quarterly of Applied Mathematics, Vol. XV, No. 4, 1958, p. 367-380.
22. Itao, K. and Crandall, S.H., "Natural Modes and Natural Frequencies of Uniform, Circular, Free-edge Plates," Transactions of the ASME, Journal of Applied Mechanics, Vol. 46, June 1979, p. 448-453.
23. Xing Guangqian and Bainum, Peter M., "The Optimal LQG Digital Control of Orbiting Large Flexible Beams," AAS/AIAA Astrodynamics Specialist Conference, Kalispel, Montana, August 10-13, 1987, Paper No. AAS 87-418; also in The Journal of the Astronautical Sciences, Vol. 37, No. 1, 1989, pp. 59-78.
24. Armstrong, E.S., ORACLS, A Design System for Linear Multi-variable Control, Marcel Dekker, Inc., New York and Basel, 1980.

25. Kalman, R.E., Ho, Y.C. and Narendra, K.S., "Controllability of Linear Dynamical System," Contributions to Differential Equations, Vol. 1, No. 2, 1961, pp. 182-213.
26. Tomovic, R., "Controllability, Invariancy, and Sensitivity," Proc. Third Allerton Conference, 1965, pp. 17-26.
27. Johnson, C.D., "Optimization of a Certain Quality of Complete Controllability and Observability for Linear Dynamical Systems," A.S.M.E. Trans. J. Basic Engrg., Vol. 191, Ser. D, 1969, pp. 228-238.
28. Muller, P.C. and Weber, H.I., "Analysis and Optimization of Certain Qualities of Controllability and Observability for Linear Dynamical Systems," Automatica, Vol. 8, 1972, pp. 237-246.
29. Viswanathan, C.N., Longman, R.W. and Likins, P.W., "A Definition of the Degree of Controllability - A Criterion for Actuator Placement," Proceedings of the Second VPI&SU/ AIAA Symposium on Dynamics and Control of Large Flexible Spacecraft, Blacksburg, VA, June 1979, pp. 369-381.
30. Athans, M. and Falb, P.L., Optimal Control: An Introduction to the Theory and Its Applications, McGraw-Hill Book Co., New York, 1966.
31. Ogata, K., Discrete-Time Control Systems, Prentice Hall, Inc., New Jersey, 1987.
32. Santini, P., "Stability of Flexible Spacecrafts," Acta Astronautica, Vol. 3, 1977, pp. 685-713.
33. Bainum, P.M., Reddy, A.S.S.R., Krishna, R. and Hamer, H.A., "Control of a Large Flexible Platform in Orbit," Journal of Guidance and Control, Vol. 4, No. 6, November-December 1981, pp. 642-649.
34. Warburton, G.B., "The Vibration of Rectangular Plates," Proceeds. Institute of Mechanical Engineers, Vol. 168, No. 12, 1954, pp. 371-394.
35. Warburton, G.B., "Response Using the Raleigh-Ritz Method," Earthquake Engineering and Structural Dynamics, Vol. 7, 1979, pp. 327-334.
36. Leissa, A.W., "Vibration of Plates," NASA SP-160, NASA, Washington, DC, 1969, pp. 87-110.
37. Logcher, R.D., Connor, Jr., J.J. and Nelson, M.F., "ICES-STRUDEL-II, Engineering Users Manual, Vol. 2, 2nd Ed., Massachusetts Institute of Technology, December 1973.

38. GTSTRU DL User's Manual," GTICES Systems Laboratory, Georgia Institute of Technology, Atlanta, GA, Rev. J, April 1988.
39. Bainum, P.M., Reddy, A.S.S.R., Krishna, R. and James, P.K., "The Dynamics and Coantrol of Large Flexible Space Structures - III", Final Report, NASA Grant NSG-1414, Suppl. 2, Part B: Shape and Orientation Control of a Platform in Orbit using Point Acutators, Howard University, June, 1980.

APPENDIX

SEVERAL PROOFS FOR THE DEGREE OF CONTROLLABILITY PROBLEM

1. The Proof of Invariability of the Degree of Controllability Under Orthogonal Linear Transformation

It is supposed that the linear discrete-time system is as follows:

$$x_k = \phi x_{k-1} + \Gamma u_{k-1} \quad (A1)$$

let $x_k = L \tilde{x}_k$ (A2)

where

L = orthogonal linear transformation

The equation of the new system after linear transformation is as follows:

$$\tilde{x}_k = \tilde{\phi} \tilde{x}_{k-1} + \tilde{\Gamma} u_{k-1} \quad (A3)$$

where

$$\tilde{\phi} = L^{-1} \phi L = L^T \phi L, \quad L^{-1} \Gamma = L^T \Gamma = \tilde{\Gamma}$$

The controllability matrix for the system (A1) is

$$P_c = (\Gamma : \phi \Gamma : \phi^2 \Gamma : \dots : \phi^{n-1} \Gamma) \quad (A4)$$

The degree of controllability matrix W_c is

$$W_c = P_c P_c^T = \Gamma \Gamma^T + \phi \Gamma \Gamma^T \phi^T + \dots + \phi^{n-1} \Gamma \Gamma^T (\phi^{n-1})^T$$

The controllability matrix for the system (A3) is

$$\begin{aligned} \tilde{P}_c &= (\tilde{\Gamma} : \tilde{\phi} \tilde{\Gamma} : \tilde{\phi}^2 \tilde{\Gamma} : \dots : \tilde{\phi}^{n-1} \tilde{\Gamma}) = (L^{-1} \Gamma : L^{-1} \phi L L^{-1} \Gamma : \dots : \\ &\quad (L^{-1} \phi L)(L^{-1} \phi L) \dots (L^{-1} \phi L) L^{-1} \Gamma) \\ &= L^{-1} (\Gamma : \phi \Gamma : \dots : \phi^{n-1} \Gamma) = L^{-1} P_c \end{aligned}$$

The degree of controllability matrix for the system (A3), \tilde{W}_c , is as follows:

$$\tilde{W}_c = \tilde{P}_c \tilde{P}_c^T = L^{-1} P_c P_c^T L \quad (A5)$$

As we know, the eigenvalues of a matrix are invariant under a similarity transformation, i.e.,

$$\Lambda(\tilde{W}_c) = \Lambda(L^{-1} P_c P_c^T L) = \Lambda(P_c P_c^T) = \Lambda(W_c) \quad (A6)$$

Therefore, the degree of controllability is also invariant under a similarity transformation, i.e.,

$$\mu_i(\tilde{W}_C) = \mu_i(W_C) \quad (i = 1, 2, 3) \quad (A7)$$

2. The Proof of the General Properties (a) - (d) for the Degree of Controllability $\mu_i(W_C)$ ($i = 1, 2, 3$)

(1) The case for μ_1

It is evident that the properties (a) - (c) for μ_1 are true. What we need to prove is property (d). That the property (d) is true is due to the following facts.

If $W_C = W_{C1} + W_{C2}$; $W_{C1}, W_{C2} \in W_C^*$, then

$$\begin{aligned} \mu_1(W_C) &= \lambda_{\min}(W_C) = \min_{\substack{\|x\|=1 \\ x \in R^n}} \langle W_C x, x \rangle = \min_{\|x\|=1} \{ \langle W_{C1} x, x \rangle \\ &\quad + \langle W_{C2} x, x \rangle \} > \min_{\|x\|=1} \langle W_{C1} x, x \rangle + \min_{\|x\|=1} \langle W_{C2} x, x \rangle \\ &= \lambda_{\min}(W_{C1}) + \lambda_{\min}(W_{C2}) = \mu_1(W_{C1}) + \mu_1(W_{C2}) \end{aligned} \quad (A8)$$

(2) The case for μ_2

Because the trace of a positive definite symmetrical matrix is invariant under a similarity transformation, it is evident that the properties (a) - (c) are true. The proof of property (d) for μ_2 is as follows.

Based on the definition of μ_2 , what we want to prove is the following inequality:

$$\mu_2(W_C) = \frac{n}{\text{tr} W_C^{-1}} \geq \frac{n}{\text{tr} W_{C1}^{-1}} + \frac{n}{\text{tr} W_{C2}^{-1}} = \mu_2(W_{C1}) + \mu_2(W_{C2}) \quad (A9)$$

where $W_{C1}, W_{C2} \in W_C^*$, $W_C = W_{C1} + W_{C2}$

It is well known that

$$W_C^{-1} = \text{Adj} W_C / \det W_C$$

then

$$\text{tr} W_C^{-1} = \sum_{i=1}^n \det W_C(i) / \det W_C \quad (A10)$$

where $\det W_C(i)$ is the determinant of the i^{th} principal minor of the matrix W_C . Considering Eq. (A10), the inequality (A9) we want to prove will become

$$\frac{\sum_{i=1}^n \frac{\det(W_{c1}(i)+W_{c2}(i))}{\det(W_{c1}+W_{c2})}}{\sum_{i=1}^n \frac{\det W_{c1}(i)}{\det W_{c1}}} \geq \frac{\sum_{i=1}^n \frac{\det W_{c2}(i)}{\det W_{c2}}}{\sum_{i=1}^n \frac{\det W_{c1}(i)}{\det W_{c1}}} + \frac{\sum_{i=1}^n \frac{\det W_{c2}(i)}{\det W_{c2}}}{\sum_{i=1}^n \frac{\det W_{c1}(i)}{\det W_{c1}}} \quad (A11)$$

From the well known Bergstrom inequality [R1], we have

$$\frac{\det(W_{c1}+W_{c2})}{\det(W_{c1}(i)+W_{c2}(i))} \geq \frac{\det W_{c1}}{\det W_{c1}(i)} + \frac{\det W_{c2}}{\det W_{c2}(i)} \quad (A12)$$

From (A12), we have

$$\frac{\det(W_{c1}(i) + W_{c2}(i))}{\det(W_{c1} + W_{c2})} \leq \frac{1}{\frac{\det W_{c1}}{\det W_{c1}(i)} + \frac{\det W_{c2}}{\det W_{c2}(i)}}$$

then we also have

$$\sum_{i=1}^n \frac{\det(W_{c1}(i)+W_{c2}(i))}{\det(W_{c1}+W_{c2})} \leq \sum_{i=1}^n \left(\frac{\det W_{c1}}{\det W_{c1}(i)} + \frac{\det W_{c2}}{\det W_{c2}(i)} \right)^{-1} \quad (A13)$$

i.e.,

$$\left(\sum_{i=1}^n \frac{\det(W_{c1}(i)+W_{c2}(i))}{\det(W_{c1}+W_{c2})} \right)^{-1} \geq \left(\sum_{i=1}^n \left(\frac{\det W_{c1}}{\det W_{c1}(i)} + \frac{\det W_{c2}}{\det W_{c2}(i)} \right)^{-1} \right)^{-1} \quad (A14)$$

Because the $\det W_{c1}/\det W_{c1}(i)$, $\det W_{c2}/\det W_{c2}(i)$ are all real numbers, by applying the Minkowski inequality [R2]

$$\begin{aligned} & \left(\sum_{i=1}^n \left(\frac{\det W_{c1}}{\det W_{c1}(i)} + \frac{\det W_{c2}}{\det W_{c2}(i)} \right)^{-1} \right)^{-1} \geq \\ & \left(\sum_{i=1}^n \left(\frac{\det W_{c1}}{\det W_{c1}(i)} \right)^{-1} \right)^{-1} + \left(\sum_{i=1}^n \left(\frac{\det W_{c2}}{\det W_{c2}(i)} \right)^{-1} \right)^{-1} = \end{aligned} \quad (A15)$$

$$\left(\sum_{i=1}^n \frac{\det W_{c1}(i)}{\det W_{c1}} \right)^{-1} + \left(\sum_{i=1}^n \frac{\det W_{c2}(i)}{\det W_{c2}} \right)^{-1}$$

Substituting (A15) into inequality (A14), we have

$$\left(\sum_{i=1}^n \frac{\det(W_{c1}(i)+W_{c2}(i))}{\det(W_{c1}+W_{c2})} \right)^{-1} \geq \left(\sum_{i=1}^n \frac{\det W_{c1}(i)}{\det W_{c1}} \right)^{-1} + \left(\sum_{i=1}^n \frac{\det W_{c2}(i)}{\det W_{c2}} \right)^{-1} \quad (A16)$$

If the two sides of inequality (A16) are multiplied by n , the result is just what we need, (A11).

(3) The case for μ_3

It is evident that the properties (a) - (c) for μ_3 are true due directly to the definition of μ_3 . Based on the Oppenheim inequality [R1], we have

$$(\det(W_{c1} + W_{c2}))^{1/n} \geq (\det W_{c1})^{1/n} + (\det W_{c2})^{1/n} \quad (A17)$$

This is just what we want to show property (d) for μ_3 , i.e.,

$$\mu_3(W_{c1} + W_{c2}) \geq \mu_3(W_{c1}) + \mu_3(W_{c2}) \quad (A18)$$

REFERENCES FOR APPENDIX

- R1. Marshall, A.W. and Olkin, I., Inequalities: Theory of Majorization and its Applications, Academic Press, 1979, p. 478, p. 475.
- R2. Mitrinovic, D.S., Analytical Inequalities, Springer-Verlag, New York; Heidelberg. Berlin, 1970, p. 55.